CHEMISTRY OF MATERIALS

ARTICLE

pubs.acs.org/cm

Polymers with Carbazole-Oxadiazole Side Chains as Ambipolar Hosts for Phosphorescent Light-Emitting Diodes

Yadong Zhang,[†,‡] Carlos Zuniga,[†,‡] Sung-Jin Kim,[†,§] Dengke Cai,[†,§] Stephen Barlow,[†,‡] Seyhan Salman,[†,‡] Veaceslav Coropceanu,[†,‡] Jean-Luc Brédas,[†,‡] Bernard Kippelen,[†,§] and Seth Marder*[,†,‡]

[†]Center for Organic Photonics and Electronics (COPE), [‡]School of Chemistry and Biochemistry, and [§]School of Electrical and Computer Engineering, Georgia Institute of Technology, Atlanta, Georgia 30332-0400, United States

S *Supporting Information*

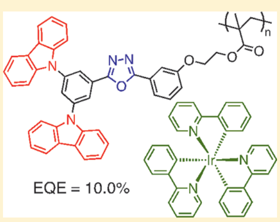

ABSTRACT: Polymethacrylates, polystyrenes, and polynorbornenes bearing 2-(3-(carbazol-9-yl)-phenyl)-5-phenyl-1,3,4-oxadiazole, 2-(4-(carbazol-9-yl)phenyl)-5-phenyl-1,3,4-oxadiazole, 2-(3,5-di-(carbazol-9-yl)phenyl)-5-phenyl-1,3,4-oxadiazole) groups linked to the polymer backbone through the 3-position of their terminal phenyl groups have been synthesized for use as solution-processable ambipolar hosts for phosphorescent light-emitting diodes. The polymers exhibit good thermal stabilities, with no weight loss below 350 °C, and have glass-transition temperatures in the range 118−209 °C. Spectroscopic, electrochemical, and quantum-chemical data for small-molecule model compounds suggest that the side chain groups are suitable hosts for a range of phosphors, including the green-emitter *fac*-tris(2-phenylpyridinato-*N,*$C^{2'}$)iridium (Ir(ppy)$_3$). Light-emitting diodes were fabricated, each with a solution-processed photo-cross-linked hole-transport layer, a solution-processed emissive layer composed of a carbazole-oxadiazole-functionalized polymethacrylate doped with Ir(ppy)$_3$, and an evaporated electron-transport layer. The polymer with 2-(3,5-(dicarbazol-9-yl)-phenyl)-5-phenyl-1,3,4-oxadiazole units in the side chain exhibited the lowest turn-on voltage (6.0 V), and the highest efficiency (external quantum efficiency of 10.0%, current efficiency of 34.1 cd/A).

KEYWORDS: oxadiazole, carbazole, light-emitting diode, phosphorescence, side-chain polymer, triplet energy

INTRODUCTION

Phosphorescent organic light-emitting diodes (OLEDs) are theoretically capable of luminescence with internal quantum efficiencies of up to 100%, fully harvesting both the singlet and the triplet excitons created by hole−electron recombination events; they have, therefore, attracted much attention for their potential applications in color displays and solid-state lighting,[1−12] largely stimulated by Forrest and Thompson's demonstration of efficient phosphorescent OLEDs using iridium(III)-based phosphors.[13] To minimize self-quenching associated with triplet−triplet annihilation,[2,14] the phosphorescent emitter is typically used at a relatively low concentration as a guest in a charge-transporting host material (alternative approaches have been, however, used in which self-quenching is minimized by dendronization of the phosphorescent center[15]).

Although host materials with either predominantly hole- or electron-transporting properties have been widely used, ambipolar hosts have potential advantages arising from more balanced injection and transport of holes and electrons. For example, more balanced carrier injection and transport leads to a broader recombination zone within the emissive layer, with a concomitant reduction of the local density of phosphor excitons and, therefore, of the rate of triplet−triplet annihilation and other triplet quenching processes.[16,17] In many cases the use of ambipolar host materials permits the fabrication of efficient OLEDs with relatively simple device architectures.[18−22] One approach to the design of ambipolar hosts is to combine known hole-transporting donor and electron-transporting acceptor functionalities, either in the same molecule, in the same polymer, or in blends of different materials. To achieve efficient energy transfer from the host to the guest, and to prevent back energy transfer from guest to host, the singlet and triplet excited-state energies of the host should generally be higher than the respective energies for the guest,[23] placing significant constraints on the design of ambipolar host materials; care must be taken that charge-transfer-type states associated with donor−acceptor interactions are sufficiently high in energy for compatibility with the phosphor of interest. However, many hosts that function well as hosts for red, green, and, in some cases, blue-green phosphors have been developed based on carbazole donors and oxadiazole acceptors: these include blends of poly(*N*-vinylcarbazole) with small-molecule or polymeric oxadiazoles,[19,20,22,24−26] copolymers of carbazole, and oxadiazole-containing monomers (in some cases also incorporating the phosphor as a monomer),[27] main-chain carbazole polymers with side-chain oxadiazoles,[28] and small molecules in which the carbazoles are linked to oxadiazole through various conjugated or nonconjugated bridging groups.[29−33] In addition, some carbazole-oxadiazole materials have been used as fluorophores or hosts for other longer-wavelength emitting fluorophores in fluorescent OLEDs.[34−36]

Received: June 2, 2011
Revised: August 2, 2011
Published: August 19, 2011

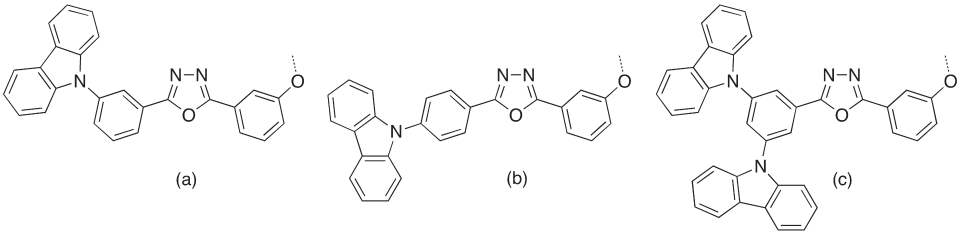

Figure 1. Carbazole-oxadiazole motifs used in this work with (a) *meta*- and (b) *para*-phenylene linkages between single carbazole and oxadiazole moieties, and (c) *meta*-linkages between two carbazoles and an oxadiazole.

We have been interested in the side-chain polymer approaches to OLEDs that potentially combine facile solution processability with morphological stability and with control of the optical and electronic properties through the choice of side chain. In this paper, we report the preparation of homopolymers based on polymethacrylate, polystyrene, and polynorbornene backbones and bearing pendant carbazole-oxadiazole transport functionalities. 2-(3-(Carbazol-9-yl)phenyl)-5-phenyl-1,3,4-oxadiazole, 2-(4-(carbazol-9-yl)phenyl)-5-phenyl-1,3,4-oxadiazole, and 2-(3,5-di(carbazol-9-yl)phenyl)-5-phenyl-1,3,4-oxadiazole groups (Figure 1a, b, and c, respectively) were chosen as ambipolar transport moieties since similar structures studied in the literature (**IV**—**VI** in Figure 3, see below) have been shown to have triplet energies suitable for use with green and blue-green phosphors.[31,33] Alkoxy groups were used to link the polymerizable groups to the terminal phenyl groups, a *meta*-linkage being chosen to avoid the π-donating alkoxy substituent significantly influencing the spectroscopic or electrochemical properties of the carbazole-oxadiazole moieties. The optical and electrochemical properties of the polymers have been assessed using the corresponding methoxy derivatives of the carbazole-oxadiazole groups as model compounds, while phosphorescent OLEDs have been fabricated using the three methacrylate polymers as hosts and *fac*-tris(2-phenylpyridinato-$N,C^{2'}$) iridium ($Ir(ppy)_3$) as a guest phosphor.

■ EXPERIMENTAL SECTION

^1H NMR and $^{13}C\{^1H\}$ NMR spectra were recorded on a 400 MHz Varian Mercury spectrometer and were referenced to Me_4Si using the residual solvent proton and carbon signals. Elemental analyses results were performed by Atlantic Microlab Inc. Mass spectra (EI) and (MALDI) were recorded on a Micromass Autospace mass spectrometer and Applied Biosystems 4700 Proteomics Analyzer mass spectrometer, respectively. The molecular weights of the polymers were estimated in tetrahydrofuran (THF) by using gel permeation chromatography using a Waters 1515 pump, a Waters 2489 UV—vis detector, a Styragel HR 5E THF 4.6 × 300 mm column, and linear poly(styrene) standards. Differential scanning calorimetry (DSC) data was obtained using a TA DSCQ200 at a heating rate of 10 °C/min from 40 to 300 °C under a nitrogen atmosphere. Thermogravimetric analysis (TGA) was performed on a NETZSCH STA 449C instrument at a heating rate of 20 °C/min from 20 to 500 °C. UV—vis absorption spectra were measured on a Hewlett-Packard 8453 spectrometer. Fluorescence spectra were recorded in dichloromethane on a Fluorolog III ISA spectrofluorimeter. The phosphorescence spectrum for **15** was recorded in 2-methyltetrahydrofuran solution at 77 K using a HORIBA Jobin Yvon Fluoromax-4P spectrofluorimeter at an excitation wavelength of 300 nm. Solution cyclic voltammetry (CV) was performed on a CH Instruments electrochemical workstation at room temperature in nitrogen-purged anhydrous THF with 0.1 M tetrabutylammonium hexafluorophosphate as a supporting electrolyte at scan rate of 50 mV/s. A glassy carbon electron was used as the working electrode a platinum wire was used as an auxiliary electrode, and a silver wire anodized with AgCl was used as a pseudoreference electrode. Potentials were referenced to ferrocenium/ferrocene ($FeCp_2^{+/0}$) by addition of ferrocene to the cell.

All polymerizations were carried out under a nitrogen atmosphere using Schlenk techniques. The solvents for radical polymerizations were purified by reflux over and distillation from CaH_2. AIBN was purified by recrystallization from ethanol. 2-Bromoethyl methacrylate,[37] 5-(5-bromopentyl)bicyclo[2,2,1]hept-2-ene (mixture of *endo*- and *exo*-isomers),[38] methyl 3-iodobenzoate (**1**),[39] methyl 3,5-diiodobenzoate (**3**),[40] (5-norbornen-2-yl)methyl *p*-tolenesulfonate,[41] and Poly-TPD-F[42,43] were synthesized according to the published procedures. THF used for free-radical polymerization was purified by reflux over, and distillation from, sodium wire. Dichloromethane for the ring-opening metathesis polymerization was obtained from an MBRAUN MB-SPS solvent purification system. Other reagents and solvents were used as received without further purification unless otherwise stated.

3-Iodobenzohydrazide (4). To methyl 3-iodobenzoate, **1** (25.0 g, 95.4 mmol) in ethanol (120 mL), was added hydrazine hydrate (50 mL). The reaction mixture was heated to reflux for 18 h. After cooling to room temperature, water (300 mL) was added. The white solid that formed was collected by filtration. The product was washed with water and dried under vacuum to give a white solid, 23.0 g (92%). ^1H NMR (400 MHz, DMSO-d_6) δ: 9.85 (s, br, 1H, NH), 8.14 (t, J = 1.6 Hz, 1H), 7.85 (dt, J = 8.0, 1.6 Hz, 1H), 7.82 (dt, J = 8.0, 1.6 Hz, 1H), 7.25 (t, J = 8.0 Hz, 1H), 4.50 (s, 2H, NH_2). $^{13}C\{^1H\}$ NMR (100 MHz, DMSO-d_6) δ: 164.73, 140.06, 135.94, 135.76, 130.98, 126.75, 95.10. MS(EI): m/z 262 (M^+). Anal. Calcd for $C_7H_7IN_2O$: C, 32.08; H, 2.69; N, 10.69. Found: C, 32.23; H, 2.61; N, 10.75.

4-Iodobenzohydrazide (5). Compound **5** (26.0 g, 87%) was synthesized from methyl 4-iodobenzoate, **2** (30.0 g, 114 mmol), using a procedure analogous to that for compound **4**. ^1H NMR (400 MHz, DMSO-d_6) δ: 9.84 (s, 1H, NH), 7.82 (d, J = 8.4 Hz, 2H), 7.59 (d, J = 8.4 Hz, 2H), 4.50 (s, 2H, NH_2). $^{13}C\{^1H\}$ NMR (100 MHz, DMSO-d_6) δ: 165.62, 137.65, 133.15, 129.37, 99.05. MS(EI): m/z 262 (M^+). Anal. Calcd for $C_7H_7IN_2O$: C, 32.08; H, 2.69; N, 10.69. Found: C, 32.30; H, 2.64; N, 10.69.

3,5-Diiodobenzohydrazide (6). Compound **6** (4.6 g, 92%) was synthesized from methyl 3,5-diiodobenzoate, **3** (5.0 g, 13 mmol), using a procedure analogous to that for compound **4**. ^1H NMR (400 MHz, DMSO-d_6) δ: 9.92 (s, 1H, NH), 8.22 (t, J = 1.6 Hz, 1H), 8.12 (d, J = 1.6 Hz, 2H), 4.53 (s, 2H, NH_2). $^{13}C\{^1H\}$ NMR (100 MHz, DMSO-d_6) δ: 163.26, 146.96, 137.04, 135.37, 96.48. MS(EI): m/z 388 (M^+). Anal. Calcd for $C_7H_6I_2N_2O$: C, 21.67; H, 1.56; N, 7.22. Found: C, 21.88; H, 1.44; N, 7.23.

3-Iodo-*N*′-(3-methoxybenzoyl)benzohydrazide (7). To a solution of **4** (10.0 g, 38.2 mmol) in a mixture of dry THF (100 mL) and dimethylformamide (DMF, 10 mL) was slowly added 3-methoxybenzoyl chloride (7.0 g, 42 mmol) at 0 °C under nitrogen, during which time a white solid appeared. After the addition was complete, the reaction mixture was allowed to warm to room temperature and then stirred for 19 h at room temperature. Pyridine (20 mL) was added, and the mixture was stirred for an additional 45 min. Water (300 mL) was then added to the reaction mixture; the white solid that formed was collected by filtration and washed with water, recrystallized from methanol, and dried under vacuum to give compound **7** as a white powder in 12.4 g (82%). ^{1}H NMR (400 MHz, DMSO-d_6) δ: 10.62 (s, 1H, NH), 10.56 (s, 1H, NH), 8.25 (t, J = 1.6 Hz, 1H), 7.96 (d, J = 8.0 Hz, 1H), 7.91 (d, J = 8.0 Hz, 1H), 7.49 (d, J = 8.0 Hz, 1H), 7.45 (d, J = 2.4 Hz, 1H), 7.41 (d, J = 8.0 Hz, 1H), 7.34 (t, J = 8.0 Hz, 1H), 7.16 (dd, J = 8.0, 2.4 Hz, 1H), 3.81 (s, 3H, OCH_3). $^{13}C\{^1H\}$ NMR (100 MHz, DMSO-d_6) δ: 166.00, 164.92, 159.67, 140.89, 136.37, 135.00, 134.24, 131.21, 130.17, 127.33, 120.17, 118.27, 113.00, 95.22, 55.78 ppm. MS(MALDI): m/z 397 (MH^+). Anal. Calcd for $C_{15}H_{13}IN_2O_3$: C, 45.47; H, 3.31; N, 7.07. Found: C, 45.24; H, 3.30; N, 6.96.

4-Iodo-*N*′-(3-methoxybenzoyl)benzohydrazide (8). Compound **8** was obtained as a white powder (7.2 g, 95%) from **5** (5.0 g, 19 mmol) and 3-methoxybenzoyl chloride (3.5 g, 21 mmol) using a procedure analogous to that used for compound **7**. ^{1}H NMR (400 MHz, DMSO-d_6) δ: 10.60 (s, 1 H, NH), 10.52 (s, 1 H, NH), 7.91 (d, J = 8.0 Hz, 2H), 7.68 (d, J = 8.0 Hz, 2H), 7.50 (d, J = 8.0 Hz, 1H), 7.45 (d, J = 2.4 Hz, 1H), 7.41 (d, J = 8.0 Hz, 1H), 7.15 (dd, J = 8.0, 2.4 Hz, 1H), 3.81 (s, 3H, OCH_3). $^{13}C\{^1H\}$ NMR (100 MHz, DMSO-d_6) δ: 166.00, 165.74, 159.67, 137.92, 134.28, 132.42, 130.17, 129.80, 120.14, 118.25, 112.97, 100.10, 55.77. MS(MALDI): m/z 397 (MH^+). Anal. Calcd for $C_{15}H_{13}IN_2O_3$: C, 45.47; H, 3.31; N, 7.07. Found: C, 45.35; H, 3.39; N, 6.95.

3,5-Diiodo-*N*′-(3-methoxybenzoyl)benzohydrazide (9). Compound **9** was obtained as white powder (5.05 g, 83%) from **6** (4.5 g, 12 mmol) and 3-methoxybenzoyl chloride (2.2 g, 13 mmol) using a procedure analogous to that used for compound **7**. ^{1}H NMR (400 MHz, DMSO-d_6) δ: 10.72 (s, 1H, NH), 10.62 (s, br, 1H, NH), 8.33 (t, J = 1.6 Hz, 1H), 8.23 (d, J = 1.6 Hz, 2H), 7.50−7.41 (m, 3H), 7.15 (m, 1H), 3.81 (s, 3H, OCH_3). $^{13}C\{^1H\}$ NMR (100 MHz, DMSO-d_6) δ: 165.91, 163.57, 159.68, 147.82, 136.23, 135.82, 134.11, 130.18, 120.17, 118.33, 112.99, 96.67, 55.79. MS(MALDI): m/z 523 (MH^+). Anal. Calcd for $C_{15}H_{12}I_2N_2O_3$: C, 34.51; H, 2.32; N, 5.37. Found: C, 34.78; H, 2.25; N, 5.42.

2-(3-Iodophenyl)-5-(3-methoxyphenyl)-1,3,4-oxadiazole (10). Compound **7** (11.0 g, 27.8 mmol) was suspended in $POCl_3$ (60.0 mL), and the reaction mixture was stirred at 100 °C. During heating the white solid starting materials dissolved to give a clear solution. After 2 h the reaction mixture was brought to room temperature and was carefully added to ice−water (1000 mL). The white solid that precipitated was collected by filtration, washed with water, and dried. The crude product was purified by column chromatography on silica gel, eluting with dichloromethane/ethyl acetate (19:1). The solid obtained after evaporation of the solvents was recrystallized from acetone/water and then dried under vacuum to give **10** as white solid (6.4 g, 61%). ^{1}H NMR (400 MHz, $CDCl_3$) δ: 8.47 (t, J = 1.6 Hz, 1H), 8.12 (dt, J = 8.0, 1.6 Hz, 1H), 7.88 (m, 1H), 7.70 (dt, J = 8.0, 1.6 Hz, 1H), 7.67 (m, 1H), 7.45 (t, J = 8.0 Hz, 1H), 7.28 (t, J = 8.0 Hz, 1H), 7.10 (m, 1H), 3.92 (s, 3H, OCH_3). $^{13}C\{^1H\}$ NMR (100 MHz, $CDCl_3$) δ: 164.79, 163.07, 159.94, 140.58, 135.46, 130.68, 130.26, 126.03, 125.68, 124.69, 119.36, 118.36, 111.59, 94.39, 55.56. MS(EI): m/z 378 (M^+). Anal. Calcd for $C_{15}H_{11}IN_2O_2$: C, 47.64; H, 2.93; N, 7.41. Found: C, 47.65; H, 2.85; N, 7.54.

2-(4-Iodophenyl)-5-(3-methoxyphenyl)-1,3,4-oxadiazole (11). Compound **11** was obtained as a white solid (5.8 g, 87%) from **8** (7.0 g, 18 mmol) by a procedure analogous to that used for compound **10**, differing only in the eluent used for column chromatography (25:1 dichloromethane/ethyl acetate). ^{1}H NMR (400 MHz, $CDCl_3$) δ: 7.86 (d, J = 8.4 Hz, 2H), 7.83 (d, J = 8.4 Hz, 2H), 7.67 (dt, J = 8.0, 1.2 Hz, 1H), 7.63 (m, 1H), 7.42 (t, J = 8 Hz, 1H), 7.07 (m, 1H), 3.88 (s, 3H, OCH_3). $^{13}C\{^1H\}$ NMR (100 MHz, $CDCl_3$) δ: 164.66, 164.00, 159.92, 138.32, 130.23, 128.21, 124.73, 123.26, 119.29, 118.26, 111.56, 98.60, 55.52. MS(EI): m/z 378 (M^+). Anal. Calcd for $C_{15}H_{11}IN_2O_2$: C, 47.64; H, 2.93; N, 7.41. Found: C, 47.77; H, 2.81; N, 7.18

2-(3,5-Diiodophenyl)-5-(3-methoxyphenyl)-1,3,4-oxadiazole (12). Compound **12** was obtained as a white solid (3.4 g, 71%) from **9** (5.0 g, 9.6 mmol) by a procedure analogous to that used for compound **10** (using the same eluent as for **10**). ^{1}H NMR (400 MHz, $CDCl_3$) δ: 8.43 (d, J = 1.6 Hz, 2H), 8.23 (t, J = 1.6 Hz, 1H), 7.71 (d, J = 8.0 Hz, 1H), 7.66 (m, 1H), 7.46 (t, J = 8.0 Hz, 1H), 7.12 (dd, J = 8.0, 2.4 Hz, 1H), 3.92 (s, 3H, OCH_3). $^{13}C\{^1H\}$ NMR (100 MHz, $CDCl_3$) δ: 165.06, 161.67, 159.98, 148.05, 134.63, 130.31, 126.95, 124.44, 119.44, 118.56, 111.66, 94.98, 55.59. MS(EI): m/z 504 (M^+). Anal. Calcd for $C_{15}H_{10}I_2N_2O_2$: C, 35.74; H, 2.00; N, 5.56. Found: C, 35.58; H, 1.92; N, 5.60.

2-(3-(Carbazol-9-yl)phenyl)-5-(3-methoxyphenyl)-1,3,4-oxadiazole (13). A mixture of **10** (3.0 g, 7.9 mmol), carbazole (1.5 g, 9.0 mmol), Cu (2.0 g, 32 mmol), and potassium carbonate (4.0 g, 29 mmol) in DMF (20.0 mL) was stirred at 150 °C for 5 h. After allowing it to cool to room temperature, the reaction mixture was diluted with THF (100 mL) and filtered. The solid residues were carefully washed with THF. The combined THF extracts were evaporated, and water (150 mL) was added; the resulting brown solid was collected by filtration. The crude product was purified by column chromatography on silica gel using dichloromethane/ethyl acetate (19:1) as eluent. The white solid obtained after evaporating the solvent was recrystallized from acetone/methanol and finally dried under vacuum to give **13** as a white solid in 3.15 g (95%) yield. ^{1}H NMR (400 MHz, $CDCl_3$) δ: 8.34 (t, J = 1.6 Hz, 1H), 8.27 (m, 1H), 8.18 (dt, J = 8.0, 0.8 Hz, 2H), 7.78 (m, 2H), 7.71−7.65 (m, 2H), 7.46−7.41 (m, 5H), 7.36−7.31 (m, 2H), 7.09 (dd, J = 8.0, 1.2 Hz, 1H), 3.89 (s, 3H, OCH_3). $^{13}C\{^1H\}$ NMR (100 MHz, $CDCl_3$) δ: 164.85, 163.84, 159.96, 140.60, 138.70, 130.85, 130.32, 130.25, 126.19, 125.84, 125.40, 124.72, 123.55, 120.45, 120.37, 119.39, 118.44, 111.52, 109.55, 55.55 (1 resonance not observed, presumably because of overlap). MS(EI): m/z 417 (M^+). Anal. Calcd for $C_{27}H_{19}N_3O_2$: C, 77.68; H, 4.59; N, 10.07. Found: C, 77.47; H, 4.51; N, 10.06.

2-(4-(Carbazol-9-yl)phenyl)-5-(3-methoxyphenyl)-1,3,4-oxadiazole (14). Compound **14** was obtained as a white solid (3.2 g, 97%) from **11** (3.0 g, 7.9 mmol) and carbazole (1.5 g, 8.97 mmol) by a procedure analogous to that used for compound **13**. ^{1}H NMR (400 MHz, $CDCl_3$) δ: 8.38 (m, 2H), 8.16 (d, J = 8.0 Hz, 2 Hz), 7.81−7.72 (m, 4H), 7.52−7.43 (m, 5H), 7.33 (m, 2H), 7.12 (m, 1H). $^{13}C\{^1H\}$ NMR (100 MHz, $CDCl_3$) δ: 164.72, 164.02, 159.99, 140.90, 140.21, 130.28, 128.58, 127.21, 126.21, 124.88, 123.76, 122.40, 120.57, 120.48, 119.33, 118.29, 111.61, 109.68, 55.55 MS(EI): m/z 417 (M^+). Anal. Calcd for $C_{27}H_{19}N_3O_2$: C, 77.68; H, 4.59; N, 10.07. Found: C, 77.71; H, 4.47; N, 10.04.

2-(3,5-Di(carbazol-9-yl)phenyl)-5-(3-methoxyphenyl)-1,3,4-oxadiazole (15). Compound **15** was obtained as white solid (0.99 g, 86%) from **12** (1.0 g, 2.0 mmol) and carbazole (1.0 g, 6.0 mmol) by a procedure analogous to that used for compound **13**, but differing in the use of toluene/ethyl acetate (97:3) as eluent and THF/methanol for recrystallization. ^{1}H NMR (400 MHz, $CDCl_3$) δ: 8.47 (d, J = 2.4 Hz, 2H), 8.16 (d, J = 8.0 Hz, 4H), 8.01 (t, J = 1.6 Hz, 1H), 7.69−7.64 (m, 2H), 7.58 (d, J = 8.0 Hz, 4H), 7.45 (m, 4H), 7.41 (t, J = 8.0 Hz, 1H), 7.34 (m, 4H), 7.08 (m, 1H), 3.87 (s, 3H, OCH_3). $^{13}C\{^1H\}$ NMR (100 MHz, $CDCl_3$) δ: 165.19, 163.30, 159.98, 140.46, 140.28, 130.31, 128.03, 127.38, 126.43, 124.49, 123.81, 123.72, 120.80, 120.60, 119.48, 118.66, 111.55, 109.52, 55.57. MS(EI): m/z 582 (M^+). Anal. Calcd for $C_{39}H_{26}N_4O_2$: C, 80.39; H, 4.50; N, 9.62. Found: C, 80.32; H, 4.41; N, 9.60.

3-(5-(3-Carbazol-9-ylphenyl)-1,3,4-oxadiazol-2-yl)phenol (16). A solution of BBr_3 (30.0 mL of a 1 M solution in dichloromethane) was added dropwise to a solution of **13** (3.0 g, 7.2 mmol) in dichloromethane (20.0 mL) at −78 °C (dry ice/acetone) under nitrogen. After addition of BBr_3 solution, the reaction was allowed to warm to room temperature and kept at room temperature for 6 h. The reaction mixture was poured into ice−water (100 mL). The dichloromethane was evaporated under reduced pressure. The white solid that formed was collected by filtration. The product was purified by recrystallization from acetone/water. After drying under vacuum, compound **16** was obtained as a white solid (2.9 g, 100%). ^{1}H NMR (400 MHz, acetone-d_6) δ: 8.89 (s, br, 1H, OH), 8.41 (m, 1H), 8.34 (m, 1H), 8.26 (m, 2H), 7.92 (m, 2H), 7.66 (m, 2H), 7.53−7.41 (m, 5H), 7.33 (m, 2H), 7.10 (m, 1H) . ^{13}C{^{1}H} NMR (100 MHz, acetone-d_6) δ: 164.71, 163.74, 157.93, 140.65, 138.61, 131.28, 130.52, 130.23, 126.29, 126.14, 125.74, 125.07, 125.06, 123.54, 120.39, 120.38, 119.01, 118.08, 113.30, 109.60. MS(EI): *m/z* 403 (M^+). Anal. Calcd for $C_{26}H_{17}N_3O_2$: C, 77.41; H, 4.25; N, 10.42. Found: C, 77.14; H, 4.15; N, 10.34.

3-(5-(4-Carbazol-9-ylphenyl)-1,3,4-oxadiazol-2-yl)phenol (17). Compound **17** was obtained as a white solid (0.97 g, 100%) from **14** (1.0 g, 2.40 mmol) by a procedure analogous to that used for compound **16**. ^{1}H NMR (400 MHz, acetone-d_6) δ: 8.91 (s, 1H, OH), 8.48 (m, 2H), 8.24 (dt, *J* = 8.0, 1.2 Hz, 2H), 7.91 (m, 2H), 7.71 (t, *J* = 1.2 Hz, 1H), 7.69 (t, *J* = 1.6 Hz, 1H), 7.56 (d, *J* = 0.8 Hz, 1H), 7.54 (t, *J* = 0.8 Hz, 1H), 7.46 (m, 3H), 7.32 (m, 2H), 7.12 (m, 1H), 3.93 (s, 3H, OCH_3). ^{13}C{^{1}H} NMR (100 MHz, acetone-d_6) δ: 165.43, 164.72, 158.87, 141.48, 141.12, 131.44, 129.41, 128.23, 127.17, 126.04, 124.56, 123.65, 121.43, 121.26, 119.88, 118.89, 114.18, 110.62. MS(EI): *m/z* 403 (M^+). Anal. Calcd for $C_{26}H_{17}N_3O_2$: C, 77.41; H, 4.25; N, 10.42. Found: C, 77.40; H, 4.19; N, 10.50.

3-(5-(3,5-Dicarbazol-9-ylphenyl)-1,3,4-oxadiazol-2-yl)phenol (18). Compound **18** was obtained as a white solid (0.92 g, 99%) from **15** (0.95 g, 1.6 mmol) by a procedure similar to that used for compound **16**, but recrystallizing from acetone/methanol. ^{1}H NMR (400 MHz, DMSO-d_6) δ: 10.01 (s, br, 1H, OH), 8.46 (d, *J* = 1.6 Hz, 2H), 8.28 (d, *J* = 8.0 Hz, 4H), 8.17 (t, *J* = 1.6 Hz, 1H), 7.66 (d, *J* = 8.0 Hz, 4H), 7.59 (d, *J* = 8.0 Hz, 1H), 7.50 (m, 5H), 7.34 (m, 5H), 7.00 (dd, *J* = 8.4, 2.4 Hz, 1H). ^{13}C{^{1}H} NMR (100 MHz, acetone-d_6) δ: 166.00, 164.37, 158.90, 141.54, 141.36, 131.55, 129.21, 128.77, 127.45, 125.90, 124.86, 124.72, 121.67, 121.44, 120.11, 119.18, 114.33, 110.79. MS(EI): *m/z* 568 (M^+). Anal. Calcd for $C_{38}H_{24}N_4O_2$: C, 80.27; H, 4.25; N, 9.85. Found: C, 80.38; H, 4.23; N, 9.79.

2-(3-(5-(3-Carbazol-9-ylphenyl)-1,3,4-oxadiazol-2-yl)phenoxy)ethyl Methacrylate (M1). To a stirred solution of **16** (0.80 g, 2.0 mmol) and 2-bromoethyl methacrylate (0.40 g, 2.1 mmol) in DMF (15 mL) was added K_2CO_3 (4.0 g, 29 mmol). After stirring at room temperature for 21 h, water (100 mL) was added and the resultant brown solid was collected by filtration. The crude product was purified by silica gel column chromatography using dichloromethane/ethyl acetate (19:1) as eluent. After removal of the solvents under reduced pressure, a viscous material was obtained; addition of methanol (120 mL) and removal under reduced pressure caused the material to solidify. The white solid product was suspended in deionized water and filtered; it was then dried in vacuum to give **M1** (0.78 g, 76%). ^{1}H NMR (400 MHz, $CDCl_3$) δ: 8.34 (m, 1H), 8.26 (m, 1H), 8.15 (dd, *J* = 8.0, 0.8 Hz, 2H), 7.78−7.66 (m, 4H), 7.42 (m, 5H), 7.31 (m, 2H), 7.10 (m, 1H), 6.12 (t, *J* = 1.2 Hz, 1H), 5.56 (m, 1H), 4.51 (m, 2H, OCH_2), 4.27 (m, 2H, OCH_2), 1.93 (t, *J* = 1.2 Hz, 3H, CH_3). ^{13}C{^{1}H} NMR (100 MHz, $CDCl_3$) δ: 167.25, 164.71, 163.88, 158.97, 140.61, 138.73, 135.86, 130.86, 130.37, 126.19, 125.85, 125.78, 125.43, 124.80, 123.56, 120.45, 120.37, 119.85, 118.88, 112.42, 109.54, 66.21, 62.84, 18.27. MS(EI): *m/z* 515.2 (M^+). Anal. Calcd for $C_{32}H_{25}N_3O_4$: C, 74.55; H, 4.89; N, 8.15. Found: C, 74.26; H, 4.83; N, 8.03.

2-(3-(5-(4-Carbazol-9-ylphenyl)-1,3,4-oxadiazol-2-yl)phenoxy)ethyl Methacrylate (M2). **M2** was synthesized from **17** (1.0 g, 2.5 mmol) and 2-bromoethyl methacrylate (0.5 g, 2.6 mmol) using the same procedure as used for **M1**. The crude product was purified by silica gel column chromatography using dichloromethane/ethyl acetate (97:3) as eluent. After removal of solvent under reduced pressure, the residue was dissolved in acetone, and the solution was added dropwise into a stirred mixture of methanol and water (3:1, 90 mL); the resultant precipitate was collected by filtration and dried in vacuum to give a white solid (0.98 g, 77%). ^{1}H NMR (400 MHz, $CDCl_3$) δ: 8.37 (d, *J* = 8.0 Hz, 2H), 8.14 (dd, *J* = 8.0, 0.8 Hz, 2H), 7.78−7.72 (m, 4H), 7.50−7.41 (m, 5H), 7.31 (m, 2H), 7.12 (dd, *J* = 8.0, 2.4 Hz, 1H), 6.16 (d, *J* = 0.4 Hz, 1H, C═C−H), 5.59 (t, *J* = 0.8 Hz, 1H, C═C−H), 4.55 (t, *J* = 4.8 Hz, 2H, OCH_2), 4.33 (t, *J* = 4.8 Hz, 2H, OCH_2), 1.96 (s, 3H, CH_3). ^{13}C{^{1}H} NMR (100 MHz, $CDCl_3$) δ: 167.28, 164.57, 164.06, 140.94, 140.22, 135.89, 130.40, 128.59, 127.21, 126.21, 124.97, 123.78, 122.34, 120.58, 120.47, 119.79, 118.74, 112.47, 109.87, 66.22, 62.86, 18.30. MS(EI): *m/z* 515 (M^+). Anal. Calcd for $C_{32}H_{25}N_3O_4$: C, 74.55; H, 4.89; N, 8.15. Found: C, 74.29; H, 4.79; N, 8.13.

2-(3-(5-(3,5-Dicarbazol-9-ylphenyl)-1,3,4-oxadiazol-2-yl)phenoxy)ethyl Methacrylate (M3). **M3** was synthesized from **18** (0.70 g, 1.2 mmol) and 2-bromoethyl methacrylate (0.25 g, 1.3 mmol) by the same procedure for **M1**. The crude product was purified by silica gel column chromatography using dichloromethane/ethyl acetate (19:1) as eluent. After removal of solvent, the residue was dissolved in THF (10 mL); addition of methanol (120 mL) to this stirred solution gave a precipitate which was collected by filtration and dried under vacuum to give a white solid (0.70 g, 84%). ^{1}H NMR (400 MHz, $CDCl_3$) δ: 8.47 (d, *J* = 1.6 Hz, 2H), 8.16 (d, *J* = 8.0 Hz, 4H), 8.01 (d, *J* = 1.6 Hz, 1H), 7.71 (dt, *J* = 8.0, 1.6 Hz, 1H), 7.67 (m, 1H), 7.57 (d, *J* = 8.4 Hz, 4H), 7.49−7.40 (m, 5H), 7.34 (m, 4H), 7.10 (m, 1H), 6.11 (t, *J* = 1.2 Hz, 1H), 5.55 (m, 1H), 4.49 (t, *J* = 4.4 Hz, 2H, OCH_2), 4.29 (t, *J* = 4.4 Hz, 2H, OCH_2), 1.92 (t, *J* = 1.2 Hz, 3H, CH_3). ^{13}C{^{1}H} NMR (100 MHz, $CDCl_3$) δ: 167.24, 165.05, 163.35, 159.01, 140.51, 140.32, 135.85, 130.43, 128.12, 127.36, 126.43, 126.16, 124.60, 123.84, 123.77, 120.82, 120.61, 119.95, 119.09, 112.50, 109.52, 66.24, 62.81, 18.26. MS(FAB): *m/z* 680 (M^+). Anal. Calcd for $C_{44}H_{32}N_4O_4$: C, 77.63; H, 4.74; N, 8.23. Found: C, 77.49; H, 4.69; N, 8.21.

2-(3-Carbazol-9-ylphenyl)-5-(3-(4-vinylbenzyloxy)phenyl)-1,3,4-oxadiazole (M4). To a stirred solution of **16** (3.0 g, 7.4 mmol) and 1-(chloromethyl)-4-vinylbenzene (1.3 g, 8.5 mmol) in DMF (40 mL) was added K_2CO_3 (12.0 g, 86.8 mmol) at room temperature. After stirring for 48 h, water (200 mL) was added; the resulting precipitate was collected by filtration, washed with water and methanol, and dried under reduced pressure. The crude product was purified by silica gel column chromatography using dichloromethane/ethyl acetate (19:1) as eluent. After removal of solvent under reduced pressure, the resulting solid was transferred to a filter with methanol and dried in vacuum to give a white solid (3.72 g, 96%). ^{1}H NMR (400 MHz, $CDCl_3$) δ: 8.32 (m, 1H), 8.26 (m, 1H), 8.17 (dd, *J* = 8.0, 1.2 Hz, 2H), 7.78−7.69 (m, 4H), 7.44−7.39 (m, 9H), 7.30 (m, 2H), 7.12 (m, 1H), 6.68 (dd, *J* = 17.6, 11.2 Hz, 1H, C═C−H), 5.72 (dd, *J* = 17.6, 0.8 Hz, 1H, C═C−H), 5.23 (dd, *J* = 11.2, 0.8 Hz, 1H, C═C−H), 5.11 (s, 2H, OCH_2). ^{13}C{^{1}H} NMR (100 MHz, $CDCl_3$) δ: 164.77, 163.83, 159.06, 140.61, 138.71, 137.49, 136.30, 135.78, 130.84, 130.31, 127.73, 126.44, 126.19, 125.81, 125.40, 124.75, 123.56, 120.44, 120.38, 119.65, 119.07, 114.22, 112.70, 109.54, 104.96, 70.00. MS(EI): *m/z* 519 (M^+). Anal. Calcd for $C_{35}H_{25}N_3O_2$: C, 80.90; H, 4.85; N, 8.09. Found: C, 80.71; H, 4.85; N, 8.03.

2-(3,5-Dicarbazol-9-ylphenyl)-5-(3-(4-vinylbenzyloxy)phenyl)-1,3,4-oxadiazole (M5). **M5** was synthesized starting from **18** (3.0 g, 5.3 mmol) and 1-(chloromethyl)-4-vinylbenzene (1.0 g, 6.6 mmol) using the same procedure as used for **M4**. The crude product was purified by silica gel column chromatography using dichloromethane/ethyl acetate (39:1) as eluent. After removal of solvent under reduced pressure, the residue was dissolved in dichloromethane; this solution was added dropwise into stirred methanol (100 mL), and the resultant precipitate was collected by filtration and dried under vacuum to give a white solid (2.45 g, 68%). ^{1}H NMR (400 MHz, $CDCl_3$) δ: 8.46 (d, *J* = 2.0 Hz, 2H), 8.17 (dd, *J* = 8.0, 0.8 Hz, 4H), 8.01 (t, *J* = 2.0 Hz, 1H), 7.72−7.70 (m, 2H), 7.58 (d, $J = 8.0$ Hz, 4H), 7.50−7.33 (m, 13H), 7.14 (m, 1H), 6.66 (dd, $J = 17.6, 11.2$ Hz, 1H, C═C−H), 5.70 (dd, $J = 17.6, 0.8$ Hz, 1H, C═C−H), 5.30 (dd, $J = 11.2, 0.8$ Hz, 1H, C═C−H), 5.11 (s, 2H, OCH_2). $^{13}C\{^1H\}$ NMR (100 MHz, $CDCl_3$) δ: 165.09, 163.28, 159.07, 140.47, 140.31, 137.47, 136.27, 135.73, 130.36, 128.04, 127.68, 127.37, 126.46, 126.42, 124.53, 123.82, 123.70, 120.81, 120.60, 119.73, 119.31, 114.21, 112.72, 109.51, 70.00. MS(FAB): m/z 684 (M^+). Anal. Calcd for $C_{47}H_{32}N_4O_2$: C, 82.44; H, 4.71; N, 8.18. Found: C, 82.18; H, 4.71; N, 8.20.

2-(3-Carbazol-9-ylphenyl)-5-(3-(5-(bicyclo[2,2,1]hept-5-en-2-ylmethoxy)phenyl)-1,3,4-oxadiazole (Mixture of *endo* and *exo* Isomers) (M6). To a stirred solution of **16** (1.0 g, 2.5 mmol) and (5-norbornen-2-yl)methyl *p*-toluenesulfonate (mixture of *endo* and *exo* isomers) (0.8 g, 3 mmol) in DMF (20 mL) was added Cs_2CO_3 (1.6 g, 4.9 mmol) at room temperature. The reaction was heated to 100 °C for 3 h; after the reaction mixture was cooled to room temperature, water (120 mL) was added, and the resultant brown solid product was collected by filtration, and purified by silica gel column chromatography using toluene/ethyl acetate (19:1) as eluent. After removal of solvents, the residue was dissolved in acetone (3.0 mL); the solution was added dropwise into a stirred mixture of methanol and water (3:1, 100 mL) and the resulting white precipitate was collected by filtration and dried under vacuum to give a white solid (1.07 g, 85%). ^1H NMR (400 MHz, $CDCl_3$) δ: 8.34 (t, $J = 1.2$ Hz, 1H), 8.27 (m, 1 Hz), 8.17 (d, $J = 8.0$ Hz, 2H), 7.81−7.76 (m, 2H), 7.70−7.61 (m, 2H), 7.46−7.31 (m, 7H), 7.07 (m, 1H), 6.19−5.95 (m, 2H, C═C−H), 4.10 (dd, $J = 8.8, 6.0$ Hz, 0.6H, 0.3 × OCH_2), 3.92 (t, $J = 8.8$ Hz, 0.4H, 0.2 × OCH_2), 3.78 (dd, $J = 8.8, 6.0$ Hz, 0.4H, 0.2 × OCH_2), 3.62 (t, $J = 8.8$ Hz, 0.6H, 0.3 × OCH_2), 3.05 (s, br, 0.4H), 2.86 (m, br, 1.6H), 2.57 (m, 1H), 1.92 (m, 1H), 1.50−1.24 (m, 3H), 0.65 (m, 1H). $^{13}C\{^1H\}$ NMR (100 MHz, $CDCl_3$) δ: 164.91, 163.81, 163.83, 159.55, 140.62, 138.71, 137.65, 136.88, 136.36, 132.26, 130.83, 130.31, 130.28, 130.21, 130.16, 126.19, 125.85, 125.42, 124.68, 124.63, 123.56, 120.45, 120.37, 119.23, 119.13, 118.84, 118.81, 112.28, 112.23, 109.55, 72.55, 71.75, 49.41, 45.04, 43.86, 43.68, 42.21, 41.58, 38.52, 38.30, 29.60, 28.98. MS(EI): m/z 509 (M^+). Anal. Calcd for $C_{34}H_{27}N_3O_2$: C, 80.13; H, 5.35; N, 8.25. Found: C, 80.00; H, 5.33; N, 8.19.

2-(4-Carbazol-9-ylphenyl)-5-(3-(5-(bicyclo[2,2,1]hept-5-en-2-yl)pentyloxy)phenyl)-1,3,4-oxadiazole (Mixture of *endo* and *exo* Isomers) (M7). To a solution of **17** (0.90 g, 2.2 mmol) and 5-(5-bromopentyl)bicyclo[2,2,1]hept-2-ene (mixture of *endo* and *exo* isomers) (0.74 g, 3.0 mmol) in DMF (10.0 mL) was added K_2CO_3 (5.0 g, 36 mmol) at room temperature with stirring. After the reaction was carried out at room temperature for 24 h, water (150 mL) was added and the resulting brown semisolid product was obtained by filtration. The crude product was purified by silica-gel column chromatography using toluene/ethyl acetate (19:1) as eluent. After removal of solvents, acetone (3.0 mL) was added to the resulting glassy solid, which disappeared and then reappeared; methanol was added into the stirred acetone solution to complete the precipitation, and the precipitate was collected by filtration and dried in vacuum to give a white solid (0.99 g, 79%). ^1H NMR (400 MHz, $CDCl_3$) δ: 8.38 (d, $J = 8.4$ Hz, 2H), 8.15 (d, $J = 8.0$ Hz, 2H), 7.80−7.70 (m, 4H), 7.52−7.43 (m, 5H), 7.33 (m, 2H), 7.10 (dd, $J = 8.0, 1.6$ Hz, 1H), 6.11 (q, $J = 2.8$ Hz, 0.7H), 6.09 (q, $J = 2.4$ Hz, 0.3H), 6.01 (q, $J = 2.4$ Hz, 0.3H), 5.92 (q, $J = 2.8$ Hz, 0.7H), 4.06 (t, $J = 6.4$ Hz, 2H, OCH_2), 2.76 (m, br, 1.7H), 2.52 (s, br, 0.3H), 1.97 (m, 1H), 1.84 (m, 2.5H), 1.51−1.23 (m, 5H), 1.21−1.06 (m, 2.5H), 0.50 (m, 1H). $^{13}C\{^1H\}$ NMR (100 MHz, $CDCl_3$) δ: 164.76, 163.97, 159.54, 140.86, 140.20, 136.94, 132.34, 130.22, 128.55, 127.18, 126.20, 124.79, 123.75, 122.40, 120.55, 120.45, 119.10, 118.66, 112.26, 109.67, 68.31, 49.53, 45.37, 42.48, 38.65, 34.67, 32.38, 29.18, 28.37, 26.24. MS(EI): m/z 565 (M^+). Anal. Calcd for $C_{38}H_{35}N_3O_2$: C, 80.68; H, 6.24; N, 7.43. Found: C, 80.62; H, 6.15; N, 7.38.

2-(3,5-Dicarbazol-9-ylphenyl)-5-(3-(5-(bicyclo[2,2,1]hept-5-en-2-yl)pentyloxy)phenyl)-1,3,4-oxadiazole (Mixture of *endo* and *exo* Isomers) (M8). **M8** was synthesized from **18** (0.90 g, 1.6 mmol) and 5-(5-bromopentyl)-bicyclo[2,2,1]hept-2-ene (mixture of *endo* and *exo* isomers) (0.5 g, 2.1 mmol) using a procedure analogous to that used for **M7**. After purification by silica-gel column chromatography using toluene/ethyl acetate (99:1) as eluent, a glassy solid was obtained; this was dissolved in acetone (12.0 mL) and the acetone solution was added dropwise into stirred methanol (120 mL) to give a white precipitate, which was isolated by filtration and dried under vacuum to give a white solid (1.05 g, 91%). ^1H NMR (400 MHz, $CDCl_3$) δ: 8.48 (d, $J = 1.6$ Hz, 2H), 8.17 (d, $J = 8.0$ Hz, 4H), 8.02 (t, $J = 1.6$ Hz, 1H), 7.68−7.58 (m, 6H), 7.50−7.33 (m, 9H), 7.07 (dd, $J = 8.0, 2.0$ Hz, 1H), 6.09 (q, $J = 2.8$ Hz, 0.7H), 6.08 (q, $J = 2.8$ Hz, 0.3H), 6.00 (q, $J = 2.8$ Hz, 0.3H), 5.90 (q, $J = 2.8$ Hz, 0.7H), 4.00 (t, $J = 6.4$ Hz, 2H, OCH_2), 2.74 (s, br, 1.7H), 2.49 (s, br, 0.3H), 1.96 (m, 1H), 1.81 (m, 2.5H), 1.46−1.03 (m, 7.5H), 0.47 (m, 1H). $^{13}C\{^1H\}$ NMR (100 MHz, $CDCl_3$) δ: 165.24, 163.26, 159.58, 140.47, 140.31, 136.91, 132.33, 130.23, 128.02, 127.42, 126.42, 124.44, 123.81, 123.72, 120.79, 120.59, 119.25, 118.96, 112.29, 109.52, 68.34, 49.52, 45.37, 42.48, 38.64, 34.63, 32.37, 29.13, 28.34, 26.20. MS(FAB): m/z 730 (M^+). Anal. Calcd for $C_{50}H_{42}N_4O_2$: C, 82.16; H, 5.79; N, 7.67. Found: C, 82.31; H, 5.77; N, 7.68.

General Procedure for Free-Radical Polymerization of Methacrylate Monomers. A Schlenk flask was charged with monomer (ca. 0.15 M **M1**, **M2**, or **M3**), AIBN (0.015 equiv), and dry THF. The polymerization mixture was purged with nitrogen to remove oxygen, sealed under nitrogen, and heated to 60 °C with stirring for 3 d. After allowing to cool to room temperature, the polymer was precipitated from the reaction mixture with ethanol and collected by filtration, redissolved in dichloromethane, and reprecipitated with ethanol again; this dissolution/precipitation procedure was repeated an additional three times. The product from the final precipitation was then dried under vacuum to give a white solid.

Polymer P1. Yield: 0.46 g (92%). ^1H NMR (400 MHz, $CDCl_3$) δ: 8.06 (s, br, 1H), 7.93 (m, br, 2H), 7.44 (s, br, 1H), 7.22 (m, br, 8H), 7.10 (s, br, 2H), 6.81 (m, br, 2H), 4.04 (m, br, 4H), 1.82 (s, br, 2H), 1.00 (m, br, 3H). Anal. Calcd for $(C_{32}H_{25}N_3O_4)_n$: C, 74.55; H, 4.89; N, 8.15. Found: C, 73.95; H, 4.72; N, 8.02.

Polymer P2. Yield: 0.47 g (92%). ^1H NMR (400 MHz, $CDCl_3$) δ: 8.01 (s, br, 2H), 7.94 (s, br, 2H), 7.43 (m, br, 4H), 7.23 (m, br, 5H), 7.13 (m, br, 2H), 6.89 (m, br, 1H), 4.12 (m, br, 4H), 1.97 (s, br, 2H), 1.00 (m, br, 3H). Anal. Calcd for $(C_{32}H_{25}N_3O_4)_n$: C, 74.55; H, 4.89; N, 8.15. Found: C, 73.64; H, 4.80; N, 7.94.

Polymer P3. Yield: 0.46 g (92%). ^1H NMR (400 MHz, $CDCl_3$) δ: 8.10 (s, br, 2H), 7.82 (s, br, 4H), 7.62 (s, br, 1H), 7.31 (m, br, 5H), 7.23 (m, br, 2H), 7.17 (s, br, 4H), 7.04 (s, br, 4H), 6.78 (m, br, 1H), 3.90 (m, br, 4H), 1.73 (m, br, 2H), 0.81 (m, br, 3H). Anal. Calcd for $(C_{44}H_{32}N_4O_4)_n$: C, 77.63; H, 4.74; N, 8.23. Found: C, 77.12; H, 4.63; N, 8.16.

General Procedure for Free-Radical Polymerization of Styrene Monomers. A Schlenk flask was charged with monomer (ca. 0.1 M **M4** or **M5**), AIBN (0.025 equiv), and dry THF. The polymerization mixture was purged with nitrogen (removal of oxygen), securely sealed under nitrogen, and heated to 60 °C with stirring for 7 d. After allowing it to cool to room temperature, the polymer was precipitated with acetone, collected by filtration, redissolved in dichloromethane, and reprecipitated with acetone again; this dissolution/precipitation (dicloromethane/acetone) procedure was repeated an additional three times. The solid from the final precipitation was dried under vacuum to give a white solid.

Polymer P4. Yield: 0.90 g (90%). ^1H NMR (400 MHz, $CDCl_3$) δ: 8.10 (s, br, 1H), 7.97 (s, br, 2H), 7.49 (s, br, 2H), 7.26 (m, br, 7H), 7.15 (s, br, 3H), 7.05 (m, br, 2H), 6.86 (m, br, 1H), 6.45 (m, br,

Chart 1

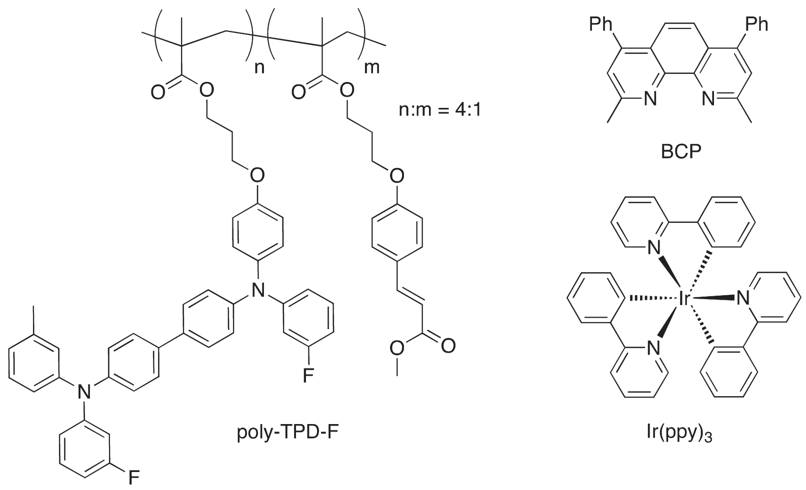

poly-TPD-F

BCP

Ir(ppy)$_3$

2H), 4.77 (s, br, 2H), 2.00−1.00 (m, br, 3H). Anal. Calcd for $(C_{35}H_{25}N_3O_2)_n$: C, 80.90; H, 4.85; N, 8.09. Found: C, 80.62; H, 4.76; N, 8.09.

Polymer P5. Yield: 0.82 g (82%). ^{1}H NMR (400 MHz, CDCl$_3$) δ: 8.17 (s, br, 2H), 7.87 (s, br, 4H), 7.68 (s, br, 1H), 7.38 (s, br, 9H), 7.09 (m, br, 4H), 6.95 (m, br, 5H), 6.29 (m, br, 2H), 4.67 (m, br, 2H), 2.00−0.60 (m, br, 3H). Anal. Calcd for $(C_{47}H_{32}N_4O_2)_n$: C, 82.44; H, 4.71; N, 8.18. Found: C, 82.36; H, 4.69; N, 8.29.

General Procedure for Ring-Opening Metathesis Polymerization of Norbornene Monomers. To a stirred dichloromethane solution of the norbornene monomer (**M6**, **M7**, or **M8**, ca. 0.1 M) was added a solution of the Grubbs first generation initiator in dichloromethane (ca. 0.008 M, 0.01 equiv) at room temperature in an inert-atmosphere glovebox. After stirring overnight, the polymerization mixture was taken out of the glovebox and ethyl vinyl ether (2 mL) was added with stirring to quench the polymerization. After stirring 30 min, the polymer was precipitated with ethanol, collected by filtration, redissolved in dichloromethane, and reprecipitated with ethanol; this dissolution/precipitation procedure was repeated two more times. Drying the product from the final precipitation under vacuum gave an off-white solid.

Polymer P6. Yield: 0.38 g (76%). ^{1}H NMR (400 MHz, CDCl$_3$) δ: 8.26 (s, br, 1H), 8.08 (s, br, 2H), 7.62 (m, br, 3H), 7.36 (s, br, 4H), 7.26 (s, br, 4H), 6.96 (m, br, 2H), 5.34 (m, br, 2H), 3.74 (m, br, 2H), 2.65 (m, br, 1H), 2.42 (m, br, 2H), 1.90 (m, br, 2H), 1.20 (m, br, 2H). Anal. Calcd for $(C_{34}H_{27}N_3O_2)_n$: C, 80.13; H, 5.34; N, 8.11. Found: C, 79.55; H, 5.22; N, 8.11.

Polymer P7. Yield: 0.41 g (82%). ^{1}H NMR (400 MHz, CDCl$_3$) δ: 8.28 (s, br, 2H), 8.08 (m, br, 2H), 7.68 (m, br, 4H), 7.38 (m, br, 3H), 7.28 (m, br, 2H), 7.26 (m, br, 2H), 7.02 (m, br, 1H), 5.26 (m, br, 2H), 3.96 (m, br, 2H), 2.87−2.72 (m, br, 1H), 2.51−2.37 (m, br, 2H), 1.85−1.75 (m, br, 4H), 1.75−1.12 (m, br, 8H). Anal. Calcd for $(C_{38}H_{35}N_3O_2)_n$: C, 80.68; H, 6.24; N, 7.43. Found: C, 79.87; H, 6.16; N, 7.30.

Polymer P8. Yield: 0.38 g (76%). ^{1}H NMR(400 MHz, CDCl$_3$) δ: 8.39 (s, br, 2H), 8.07 (s, br, 4H), 7.91 (s, br, 1H), 7.53 (d, br, 6H), 7.39 (s, br, 4H), 7.25 (s, br, 5H), 6.94 (m, br, 1H), 5.21 (m, br, 2H), 3.87 (m, br, 2H), 2.85−2.69 (m, br, 1H), 2.47−2.32 (m, br, 2H), 1.80−1.66 (m, br, 6H), 1.25−1.06 (m, br, 6H). Anal. Calcd for $(C_{50}H_{42}N_4O_2)_n$: C, 82.16; H, 5.79; N, 7.67. Found: C, 81.17; H, 5.74; N, 7.58.

OLED Device Fabrication. A 35 nm-thick hole-transport layer was fabricated by spin-coating (60 s at 1500 rpm, acceleration 10 000) a solution of the cross-linkable polymer Poly-TPD-F (Chart 1) in dry deoxygenated toluene (10 mg/mL) onto air-plasma-treated indium tin oxide (ITO) coated glass substrates with a sheet resistance of 20 Ω/□ (Colorado Concept Coatings, L.L.C.); the polymer was then photo-cross-linked by irradiating for 1.0 min with a standard broad-band UV light with a 0.7 mW/cm^2 power density. Subsequently, a 40 nm-thick emissive layer of host polymer (**P1**, **P2**, or **P3**) doped with *fac*-tris-(2-phenylpyridinato-*N*,*C*$^{2'}$) iridium, Ir(ppy)$_3$ (Chart 1) at a concentration of 6 vol. %, was spin-coated (60 s at 1000 rpm, acceleration 10 000) from a chlorobenzene solution (9.4 mg/mL polymer and 0.6 mg/mL in Ir(ppy)$_3$) on top of the insoluble photocross-linked hole-transport layer. A 40 nm-thick layer of 2,9-dimethyl-4,7-diphenyl-1,10-phenanthroline, BCP, (Chart 1, purified by gradient zone sublimation) was thermally evaporated at a rate of 0.4 Å/s and at a pressure below 1×10^{-7} Torr on top of the emissive layer to serve as an electron-transport/hole-blocking layer. Finally, 2.5 nm of lithium fluoride (LiF) as an electron-injection layer and a 200 nm-thick aluminum cathode were deposited in a vacuum chamber at a pressure below 1×10^{-6} Torr and at rates of 0.1 Å/s and 2 Å/s, respectively. A shadow mask was used for the evaporation of the metal to form five devices with an area of 0.1 cm^2 per substrate; the devices were tested immediately after cathode deposition. At no point during fabrication or testing were the devices exposed to air.

Computational Methodology. The molecular geometries of the ground singlet (S$_0$) state and lowest triplet (T$_1$) state of **13**, **14**, and **15** were optimized at the density functional theory (DFT) level using the B3LYP functional and the 6-31G(d,p) basis set, as implemented in the Gaussian03 program.[44] Ground-state geometries were confirmed to be minima of the corresponding adiabatic potential surfaces by performing additional vibrational frequency calculations. The excited-state energies and related transition dipole moments (oscillator strengths) were derived by means of the time-dependent density functional theory (TD-DFT) calculations that were carried out at the same B3LYP/6-31G(d,p) level of theory. Electronic structure calculations for Ir(ppy)$_3$ were also carried out for comparison.

RESULTS AND DISCUSSION

Preparation of Carbazole-Oxadiazole Monomers. The syntheses for the monomers are shown in Scheme 1. The iodo-substituted benzoates, **1**−**3**, reacted with hydrazine in ethanol to give iodo-substituted benzohydrazides, **4**−**6**, respectively, in good yields, which can be used for the next step without

Scheme 1

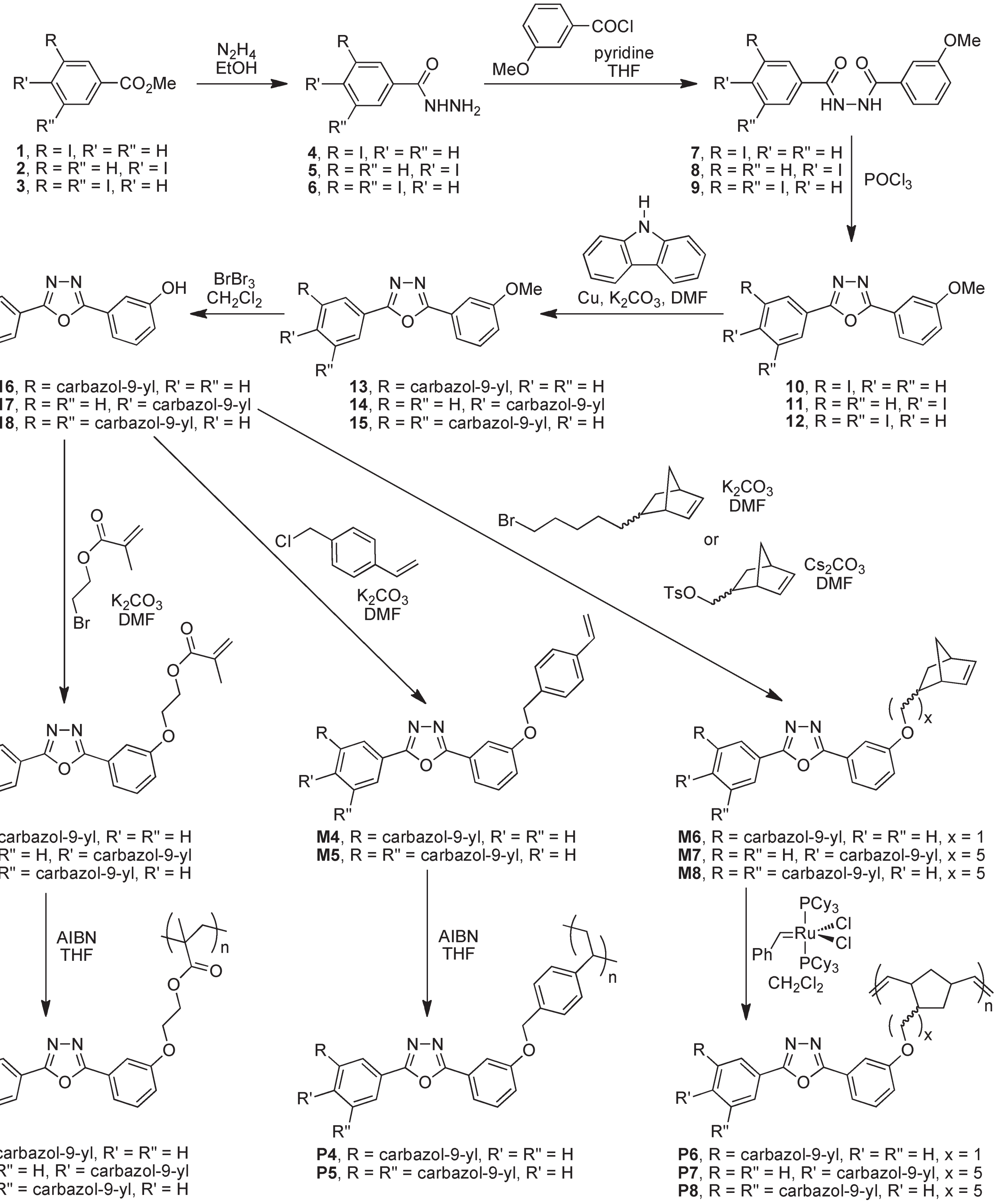

1, R = I, R' = R'' = H
2, R = R'' = H, R' = I
3, R = R'' = I, R' = H

4, R = I, R' = R'' = H
5, R = R'' = H, R' = I
6, R = R'' = I, R' = H

7, R = I, R' = R'' = H
8, R = R'' = H, R' = I
9, R = R'' = I, R' = H

10, R = I, R' = R'' = H
11, R = R'' = H, R' = I
12, R = R'' = I, R' = H

13, R = carbazol-9-yl, R' = R'' = H
14, R = R'' = H, R' = carbazol-9-yl
15, R = R'' = carbazol-9-yl, R' = H

16, R = carbazol-9-yl, R' = R'' = H
17, R = R'' = H, R' = carbazol-9-yl
18, R = R'' = carbazol-9-yl, R' = H

M1, R = carbazol-9-yl, R' = R'' = H
M2, R = R'' = H, R' = carbazol-9-yl
M3, R = R'' = carbazol-9-yl, R' = H

M4, R = carbazol-9-yl, R' = R'' = H
M5, R = R'' = carbazol-9-yl, R' = H

M6, R = carbazol-9-yl, R' = R'' = H, x = 1
M7, R = R'' = H, R' = carbazol-9-yl, x = 5
M8, R = R'' = carbazol-9-yl, R' = H, x = 5

P1, R = carbazol-9-yl, R' = R'' = H
P2, R = R'' = H, R' = carbazol-9-yl
P3, R = R'' = carbazol-9-yl, R' = H

P4, R = carbazol-9-yl, R' = R'' = H
P5, R = R'' = carbazol-9-yl, R' = H

P6, R = carbazol-9-yl, R' = R'' = H, x = 1
P7, R = R'' = H, R' = carbazol-9-yl, x = 5
P8, R = R'' = carbazol-9-yl, R' = H, x = 5

purification. The benzohydrazides, **4**−**6**, reacted with 3-methoxybenzoyl chloride to give the corresponding iodo-substituted-*N*′-(3-methoxybenzoyl)benzohydrazides **7**−**9**, which can also be used without further purification. The various iodinated derivatives of 2-(phenyl)-5-(3-methoxyphenyl)-1,3,4-oxadiazole, **10**−**12**, were obtained by heating **7**−**9** in phosphorus oxychloride. The carbazole units were then introduced under Ullmann conditions to generate the methoxy-functionalized carbazole/oxadiazole compounds **13**−**15** in excellent yields (86−96%). The corresponding phenols **16**−**18** were obtained from by the reaction of **13**−**15** with boron tribromide in dichloromethane. The monomers **M1**−**M8** were obtained in

Table 1. Molecular Weights and Thermal Properties of P1−P8

	M_w[a]	M_n[a]	PDI	T_g (°C)[b]	T_d (°C)[c]
P1	32 000	13 000	2.5	132	375
P2	46 000	17 000	2.7	141	376
P3	45 000	16 000	2.8	190	400
P4	29 000	19 000	1.5	150	385
P5	25 000	16 000	1.6	209	414
P6	66 000	46 000	1.4	138	383
P7	50 000	30 000	1.6	118	390
P8	60 000	35 000	1.7	160	412

[a] Molecular weights estimated by GPC using polystyrene standards. [b] Measured by DSC at heating rate of 10 °C/min. [c] Measured by TGA at heating rate of 20 °C/min.

good yields (67−96%) by nucleophilic substitution reactions between the phenols, **16**−**18**, and the appropriate methacrylate, styrene, or norbornene-functionalized alkyl bromide or tosylate.

Preparation and Characterization of Carbazole-Oxadiazole Polymers. The syntheses of homopolymers **P1**−**P8** are also shown in Scheme 1. The methacrylate polymers, **P1**−**P3**, and styrene polymers, **P4**−**P5**, were obtained by thermal (60 °C) free-radical polymerization of the corresponding monomers in THF in inert atmosphere, using 1.5 and 2.5 mol % of 2,2′-azobisisobutyronitrile (AIBN) as an initiator for methacrylate and styrene polymerizations, respectively. Methacrylate polymers were obtained in high yields (>90%) after reaction for 3 days, while relatively low yields of polystyrenes were obtained in the same time; good yields (>80%) of polystyrenes were, however, obtained after reaction for 7 days. Poly(norbornene)s **P6**−**P8** were synthesized in good yield (>80%) by ring-opening metathesis polymerization (ROMP) of the corresponding monomers in dichloromethane using 1.0 mol % of the Grubbs first generation initiator in a glovebox at room temperature. All the polymers were purified by repeated dissolution and precipitation and were characterized by ^{1}H NMR spectroscopy, elemental analysis, and gel-permeation chromatography (GPC). The number-average and weight-average molecular weights, M_n and M_w respectively, determined against polystyrene standards, are summarized in Table 1. The number-average molecular weights are smaller for the polymers obtained from free-radical polymerization, **P1**−**P5**, than for the ROMP polymers, **P6**−**P8**. The polydispersity indices (PDI = M_w/M_n) of the polymers with methacrylate backbones fall in the range 2.5−2.8, while the styrene- and norbornene-based polymers have narrower molecular-weight distributions with PDIs of 1.4−1.7. The number-average degrees of polymerization suggested by the GPC data for the poly(norbornene)s fall in the range 47−90, thus, in some cases falling only a little short of the value of 100 expected from the initiator/monomer ratio employed.

Thermal Properties. The thermal stabilities of the polymers were investigated by the thermal gravimetric analysis (TGA) under nitrogen (see Supporting Information, Figure S1). The decomposition temperatures (T_d), defined as the temperatures at which 5% weight loss was observed at a heating rate of 20 °C/min, are summarized in Table 1 and suggest all have reasonably good thermal stability. The decomposition temperatures seem to be influenced by the choice both of the carbazole-oxadiazole pendant group and of the backbone: for a given side chain the polymethacrylates show slightly lower decomposition temperatures than the corresponding polystyrenes and polynorbornenes, while the polymers (**P3**, **P5**, **P8**) derived from the bis(carbazole)-oxadiazole phenol **18** show somewhat higher decomposition temperatures than comparable polymers with one carbazole in the pendant group (derived from phenols **16** and **17**). The polymers were also studied using differential scanning calorimetry (DSC, see Supporting Information, Figure S2); in each case the only events detected were glass transitions, suggesting that these materials may form amorphous films. The three polymers derived from bis(carbazole)-oxadiazole phenol **18** exhibit higher glass-transition temperatures (T_g) that those from **16** and **17**, with the highest value being observed for the polystyrene **P5**.

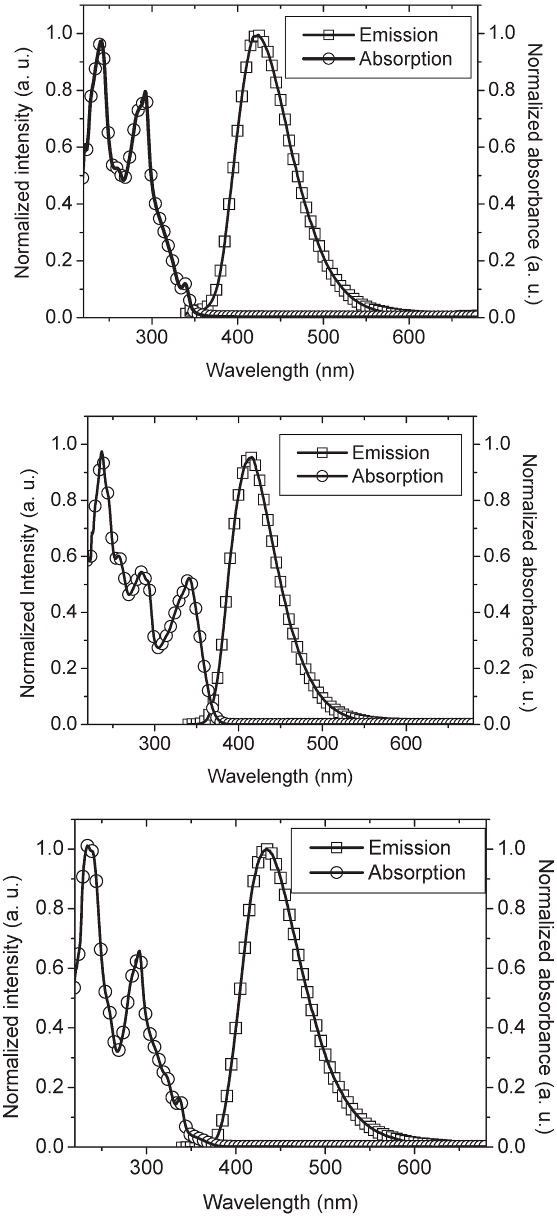

Figure 2. Normalized absorption and fluorescence spectra of **13** (top), **14** (middle), and **15** (bottom) in dichloromethane.

Photophysical Properties. The optical properties of the three carbazole-oxadiazole groups used (Figure 1) were compared using the intermediates **13**, **14**, and **15** as model compounds. Absorption

Table 2. Experimental and Quantum-Mechanical Optical Data for 13, 14, 15, and $Ir(ppy)_3$

	experimental							theoretical transition energies (eV) (oscillator strengths in parentheses)		
	absorption[a]			fluorescence[a]		phosphorescence[b]				
	λ_{max} (nm)	E_{max} (eV)	E_{onset} (eV)	λ_{max} (nm)	E_{max} (eV)	$\lambda_{0,0}$ (nm)	$E_{0,0}$ (eV)	vert. $S_0 \rightarrow S_1$[c]	vert. $S_0 \rightarrow T_1$[c]	E_T[d]
13	241, 292, 339	5.15, 4.25, 3.66	3.46	424	2.92			3.25 (0.01)	2.74	2.60
14	237, 284, 341	5.23, 4.37, 3.64	3.26	414	3.00			3.26 (0.4)	2.65	2.52
15	234, 292, 337	5.30, 4.25, 3.68	3.31	434	2.86	456	2.72	3.10 (0.02)	2.71	2.59
$Ir(ppy)_3$								2.80 (0.002)	2.52	2.36

[a] In CH_2Cl_2 at room temperature. [b] Absorption maxima for the highest energy feature in a spectrum recorded in 2-methyltetrahydrofuran at 77 K and taken as an estimate of the adiabatic triplet energy. [c] TD-DFT/B3LYP estimates of the vertical transition energies at ground-state (S_0) geometry for $S_0 \rightarrow S_1$ and $S_0 \rightarrow T_1$ transitions. [d] ΔSCF estimates of adiabatic energies of the first triplet state.

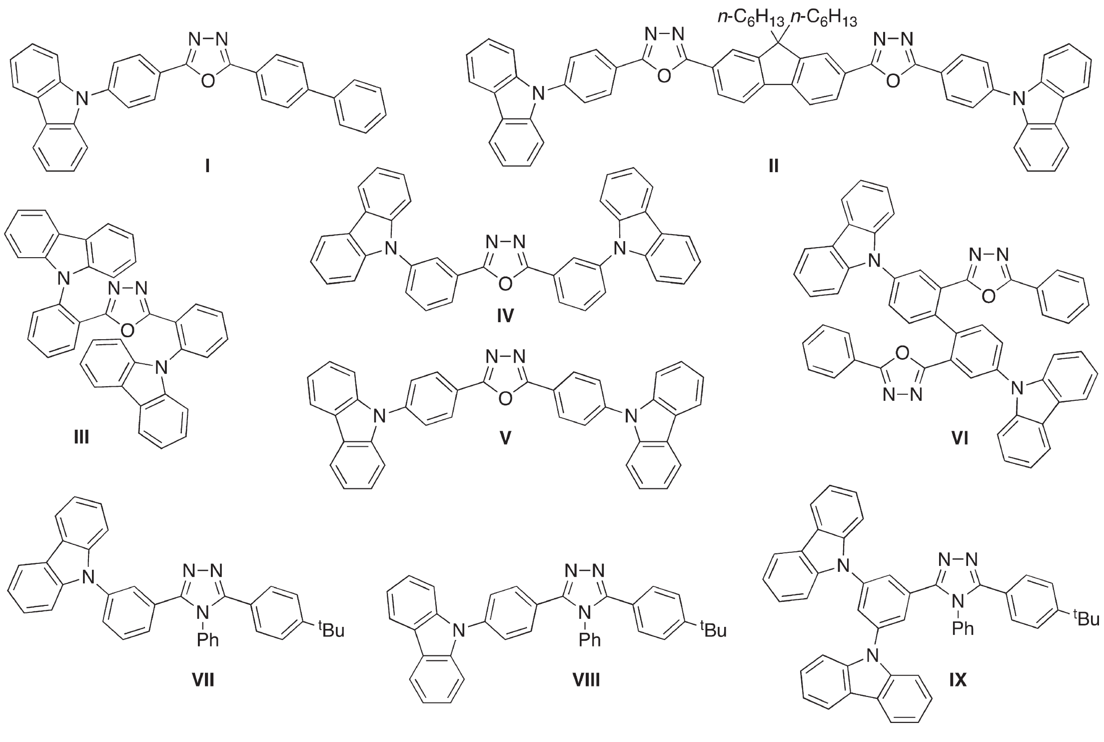

Figure 3. Some small-molecule carbazole-oxadiazole and carbazole-triazole compounds studied in the literature.

and fluorescence spectra obtained in dilute dichloromethane solution are shown in Figure 2; the absorption and emission maxima are listed in Table 2. In all three compounds the lowest energy distinct absorption maxima are at about 340 nm (ca. 3.6 eV). Maxima at similar wavelengths have been previously reported for other carbazole-oxadiazole molecules with similar structural motifs including **I**–**VI** (Figure 3, values range from 338 to 342 nm, except for **II**, for which the maximum is reported at 361 nm).[31–33,35,36] 2,5-Diphenyl-1,3,4-oxadiazole absorbs at much shorter wavelength (284 nm, 4.37 eV in chloroform),[31] while carbazole and *N*-phenylcarbzole have weak vibronically structured absorptions in the same region as the maxima observed for the present compounds (341 and 333 nm, respectively, in chloroform).[45,46] For compounds **13** and **15**, in which the carbazole(s) and oxadiazole are linked by *meta*-phenylene bridges (motifs (a) and (c) in Figure 1) the low-energy absorption is weak relative to the other shorter wavelength absorptions, whereas the lowest energy band of *para*-phenylene-linked **14** (motif of Figure 1b) is relatively strong, consistent with what is seen in comparing other *meta*- and *para*-linked donor–acceptor systems, including the closely related carbazole-oxadiazole derivatives **IV** and **V**[33] and the carbazole-triazole series **VII**–**IX** (Figure 3).[47] It should be noted that, at least for **15**, there appears to be a broad tail extending well beyond the sharp feature giving rise to the lowest resolvable maximum, suggesting the possibility of more than one weak low-energy transition (see below).

TD-DFT calculated energies for the $S_0 \rightarrow S_1$ transition of isolated gas-phase molecules are somewhat overestimated compared to the experimental absorption maxima, but, consistent with experiment, show only minor variations in transition energy between the three compounds. The TD-DFT calculations indicate that for **13**–**15** the $S_0 \rightarrow S_1$ transitions are dominated by HOMO-to-LUMO excitation. As shown in Figure 4, the HOMOs are strongly localized on the carbazole moieties, with

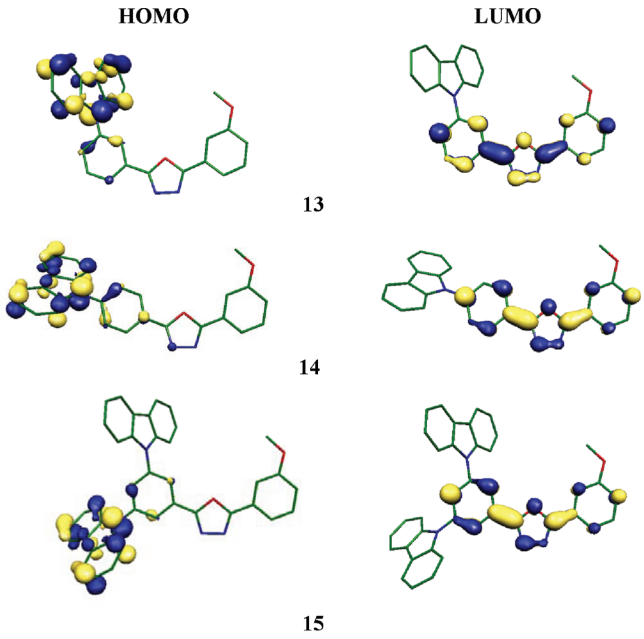

Figure 4. Illustration of the frontier molecular orbitals of **13**, **14**, and **15**.

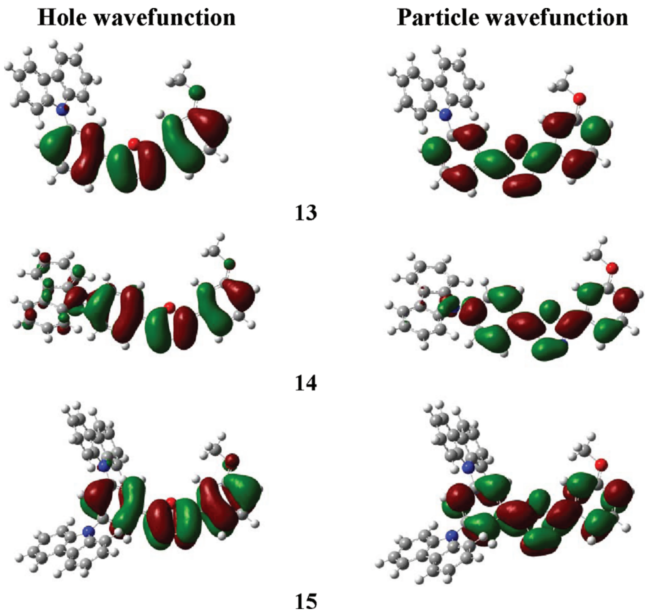

Figure 5. Illustrations of the natural transition orbitals for the T_1 state of compounds **13**, **14**, and **15**.

much smaller coefficients on the adjacent bridging phenylene group, while the LUMOs extend over the diphenyloxadiazole portion of the molecule, meaning that the first singlet excited states (S_1) in all these systems have considerable carbazole-to-diaryloxadiazole charge-transfer character.[48] The TD-DFT calculations also reproduce the variations in the relative strength of the experimental low-energy maxima; the variations in the $S_0 \rightarrow S_1$ oscillator strength (Table 1) can be attributed to the differences in HOMO−LUMO overlap on the bridging phenylene group for *para* and *meta* cases. The TD-DFT calculations indicate the presence of several weak low-energy transitions with charge-transfer character for **13** and **15**, consistent with the appearance of the long-wavelength part of the spectrum of **15** discussed above.

All three molecules show blue fluorescence with maxima in dichloromethane at 414−434 nm (2.85−3.00 eV), in a similar range to that previously reported for other related carbazole-oxadiazole molecules (416−439 nm for **II**−**VI**).[31−33,36] The emission maxima of **13**−**15** are bathochromically shifted by 0.5−0.7 eV from those of either 2,5-diphenyl-1,3,4-oxadiazole (346 nm, 3.58 eV in $CHCl_3$)[31] or *N*-phenylcarbazole (350 nm, 3.54 eV in $CHCl_3$)[45,49] and the spectra lack the resolved vibronic structure seen for those compounds, consistent with the S_1 state of the present compounds exhibiting considerable carbazole-oxadiazole charge-transfer character. As with the comparison of **IV** and **V**,[33] the *meta*-linked species in the present series exhibit the more bathochromically shifted emissions. The emissions of **15** are also significantly bathochromically shifted relative to those of the carbazole-triazoles **VII**−**IX**, where any charge-transfer-type state would be expected to be higher in energy owing to the expected effect of replacing O with the less electronegative N on the acceptor strength of the five-membered heterocycle.[47]

The phosphorescence spectrum of **15** was obtained in 2-methyltetrahydrofuran at 77 K (see Supporting Information, Figure S3). An adiabatic triplet energy of 2.72 eV was estimated from the highest energy maximum in the spectrum, identical within experimental uncertainty with the value previously reported for the other *meta*-linked carbazoles-oxadiazoles **IV** and **VI** (Figure 3),[31,33,50,51] and somewhat lower than values reported for either 2,5-diphenyl-1,3,4-oxadiazole (3.00 eV)[31] or *N*-phenylcarbazole (2.88 eV in 2-methyltetrahydrofuran).[49] DFT calculations of the adiabatic triplet energies suggest values of about 2.6 eV for **13** and **15**, close to the experimental value for **15**, and a value about 0.1 eV lower for **14**. This is consistent with results for **IV** and **V**, where the experimental triplet energy is also about 0.1 eV lower for the *para*-linked derivative **V** than for its *meta*-analogue **IV**.[33] Natural transition orbital (NTO) analyses were performed based on TD-DFT calculations carried out at the optimized T_1 geometries to obtain a better insight into the nature of the T_1 states of **13**−**15**. The obtained NTOs (Figure 5) indicate that the T_1 state in all three systems is largely localized on the diphenyl oxadiazole portion of the molecule, in contrast to the carbazole-to-oxadiazole charge-transfer character of the S_1 state. This is consistent with the observation that the experimental adiabatic triplet energies of **15** and 2,5-diphenyl-1,3,4-oxadiazole differ less from one another than do the fluorescence energies (see above). In the case of **14** both NTOs show some density on the carbazole unit, suggesting that, in this case, there is some interaction between local carbazole- and diphenyloxadiazole-localized triplet states. Presumably, it is this interaction that causes the T_1 state of **14** to be slightly lower in energy than that for the other two systems. In the context of the OLED properties investigated here, it is important to note that the experimental triplet energy of **15** is about 0.2 eV higher than that of the widely used green phosphor, $Ir(ppy)_3$ (2.4 eV in both solution and various solid matrixes),[52,53] which is used as the emitter in this work; moreover, the calculated triplet energies of all three structures are higher than that calculated for $Ir(ppy)_3$ in the same way (Table 2). **15** is also likely to be suitable for hosting the blue-green phosphor bis[(4,6-difluorophenyl)pyridinato-*N*,$C^{2'}$](picolinato-*N*,*O*) iridium, FIrpic, for which a triplet energy of about 2.6 eV is reported.[54,55]

Electrochemical Properties. As with the optical data, the methoxy-substituted carbazole-oxadiazole small molecules

Table 3. Reduction Potentials,[a] Estimated Solid-State Electron Affinities (EA)[b] and Ionization Potential (IP), and DFT/B3LYP Gas-Phase IPs and EAs of 13, 14, and 15

	$E_{1/2}^{0/-}$ (V)[a]	$EA_{(s)}$ (eV)[b,c]	$IP_{(s)}$ (eV)[d]	$EA_{(g)}$ (eV)[b] KT[e]	$EA_{(g)}$ (eV)[b] ΔSCF[f]	$IP_{(g)}$ (eV) KT[e]	$IP_{(g)}$ (eV) ΔSCF[f]
13	−2.53	2.3	5.7	1.78	0.57	5.54	6.80
14	−2.54	2.3	5.5	1.77	0.61	5.49	6.65
15	−2.33	2.5	5.8	1.92	0.84	5.53	6.64

[a] Reduction potential vs $FeCp_2^{+/0}$ in 0.1 M $^nBu_4NPF_6$ THF solution. [b] Defined as −ΔG for M + e → M^-. [c] Estimated from EA = 4.8 eV + $eE_{1/2}^{0/-}$. [d] Estimated from IP = EA + E_{onset} using E_{onset} values from Table 2; of the effects of exciton binding energy mean that these values are likely to be underestimates. [e] Estimated according to Koopmans' theorem, i.e., IP = $-E_{HOMO}$ and EA = $-E_{LUMO}$. [f] Vertical.

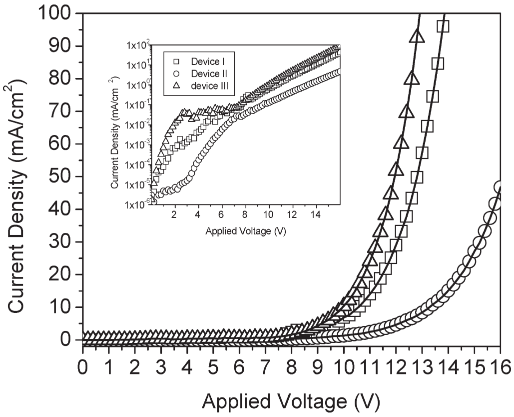

Figure 6. *J-V* characteristics of devices: I (squares), II (circles), and III (triangles) (inset shows the same data on a semilogarithmic scale).

13, **14**, and **15** were used as models for the electrochemical behavior of the corresponding side-chain polymers. Cyclic voltammograms were obtained in THF with 0.1 M tetrabutylammonium hexafluorophosphosphate as the supporting electrolyte. All three show reversible reductions (see Supporting Information, Figure S4), while the molecular oxidations (not shown) are highly irreversible, as is typical for carbazoles without 3,6 substitution because of coupling of the radical cations through these positions,[56,57] meaning values of the redox potential for this process are not easily or reliably determined. The potentials (see Table 3) are similar to those reported for other oxadiazoles (2,5-diphenyl-1,3,4-oxadiazole is reduced at −2.47 V vs $FeCp_2^{+/0}$ in acetonitrile[58,59] and the carbazole-oxadiazoles, **III**−**V**, shown in Figure 3 are reduced at about −2.3 V in THF[33]) consistent with the localization of the lowest unoccupied molecular orbitals (LUMOs) on the diphenyloxadiazole portion of the molecules. Interestingly, the *meta*- and *para*-monocarbazole derivatives, **13** and **14**, are reduced at similar potential to one another, while the bis(carbazole) derivative, **15**, is about 0.2 V more easily reduced, thus suggesting that the influence of the carbazole moieties on the redox potential of the oxadiazole moiety is largely through inductive electron withdrawal. The solid-state electron affinities (EAs) of the molecules **13**, **14**, and **15** can be estimated as 2.3−2.5 eV from the reduction potentials via the widely used relation $EA(s) \approx 4.8\ eV + eE_{1/2}^{0/-}$, where $E_{1/2}^{0/-}$ is quoted relative to ferrocenium/ferrocene.[60] Because of the irreversibility of the oxidation processes, the solid-state IPs were derived from the EA estimates and the absorption onset recognizing that the optical gap is likely to be smaller than the electrochemical gap (which, in turn, may also be smaller than the true transport gap) because of the effect of the exciton-binding energy.

IPs and EAs for isolated gas-phase molecules were also obtained from DFT calculations, both using Koopmans' theorem (KT) and ΔSCF calculations (Table 3). EAs obtained using either approach reproduce the trends seen in the experimental potentials and estimated EAs, with **15** being some 0.2 eV more readily reduced than **13** and **14**. It should be noted that the large discrepancy between the ΔSCF IPs and EAs (which are in general expected to be more accurate than those obtained at the KT level) and the experimentally estimated values is because the calculations are performed on isolated molecules and, therefore, do not account for the additional stabilizations of the ionic species by electronic polarization of the surrounding medium.[61] In the case of IPs, KT and ΔSCF calculations predict slightly different trends; however, both approaches indicate that the IPs of the present systems are very similar and differ among molecules at most by 0.14 eV.

Use as Host Materials. LEDs were fabricated to compare the polymers **P1**−**P3**, which have a common polymethacrylate backbone and the three different carbazole-oxadiazole motifs as side groups, as host matrixes for the green phosphor $Ir(ppy)_3$ (Chart 1). As in some of our previous work,[26,62,63] poly-TPD-F[42,43]—a copolymer of monomers functionalized with a bis(diarylamino)biphenyl hole-transport moiety and a photo-cross-linkable cinnamate group, shown in Chart 1—was used as a solution-processable hole-transport layer; cross-linking after 1 min of UV irradiation renders this film insoluble permitting the deposition of the polymeric emissive layer from solution. 2,9-Dimethyl-4,7-diphenyl-1,10-phenanthroline, BCP (Chart 1), was vacuum-deposited as an electron-transport layer, and finally a LiF/Al cathode was deposited to give an overall device structure ITO/poly-TPD-F(35 nm)/polymer:$Ir(ppy)_3$(6.0%)-(40 nm)/BCP(40 nm)/LiF(2.5 nm)/Al(200 nm). This device architecture has not been optimized, but is based on that of efficient green phosphorescent OLEDs with ambipolar polymeric hosts (differing from the current work in that these hosts are blends of PVK and oxadiazole side-chain polymers).[26] Devices I−III refer to those using **P1**−**P3**, respectively, as hosts.

All three devices show typical $Ir(ppy)_3$-based green emission. The behavior of devices I−III is summarized in Figures 6 and 7 and in Table 4. Devices I and III are characterized by similar turn-on voltages (defined as the voltage required to obtain a brightness of 10 cd/m^2) and external quantum efficiencies (EQEs) to one another and by fairly high maximum luminance values. These device characteristics are similar to those previously reported for similar devices using an emissive layer composed of PVK, oxadiazole side-chain polymers, and $Ir(ppy)_3$;[26,64] this is perhaps not too surprising given the use of essentially the same device architecture and given the similarity in the transport levels estimated for the emissive layers. On the other hand, device II shows a turn-on voltage about 2 V higher than those of devices I and III, along with about 6−10 times lower luminance at the same applied voltage and the lowest efficiency. These observations presumably arise from a combination of the effects of differences in hole and electron mobility values for the polymers with *meta* and *para* carbazole-oxadiazole linkages, and of

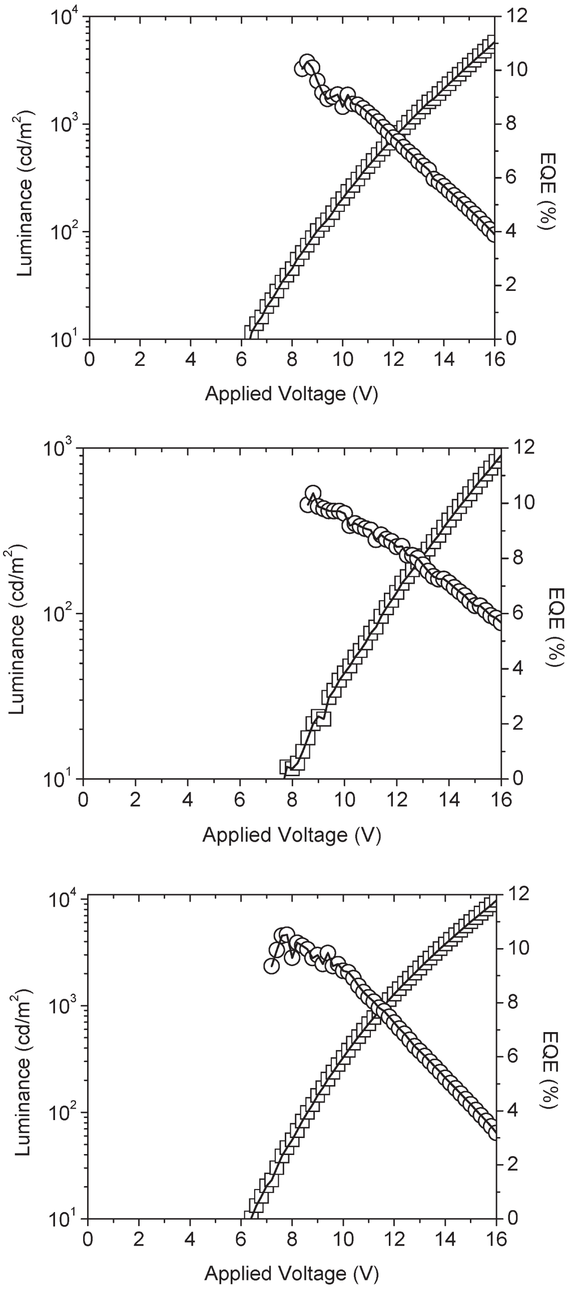

Figure 7. Luminance (squares) and external quantum efficiency (circles) as a function of the applied voltage for devices I (top), II (middle), and III (bottom).

Table 4. Performance of Green Phosphorescent OLEDs Using P1, P2, and P3 Hosts

device	host	turn-on voltage at 10 cd/m^2 (V)	maximum luminance (cd/m^2)	EQE at 100 cd/m^2 (%)	current efficiency at 100 cd/m^2 (cd/A)
I	**P1**	6.2	6500	9.6	32.9
II	**P2**	8.0	1000	8.8	30.0
III	**P3**	6.0	10000	10.0	34.1

differences in charge-injection properties, but at this point any detailed explanation of the differences in device behavior would be highly speculative. In green electrophosphorescent devices based on related small molecules **III**−**V** (Figure 3) the *para*-linked species **V** also exhibits lower efficiency than its *meta*-linked analogue **IV**, but shows a similar turn-on voltage.[33] While much higher efficiencies have been reported for devices based on related ambipolar small molecules such as **III**−**V**,[33] those devices were fully vacuum-processed whereas the current devices are partially solution-processed. As noted above, devices I and III show similar performance to devices using polymer blends as ambipolar hosts[26] and give higher efficiencies than many other solution-processed polymer green electrophosphorescent devices, including examples that we have previously reported using an emissive layer composed of a copolymer of 2,7-bis(carbazol-9-yl)fluorene host moieties and Ir(ppy)$_3$-based phosphor guests.[65] It should be noted that considerably more efficient devices (EQE up to 18.8%) have been reported that use solution-processed emissive layers based on PVK/small-molecule-oxadiazole/Ir(ppy)$_3$ blends processed onto cross-linked bis(diarylamino)-biphenyl-oxetane hole-transport layers.[24] However, compared to other solution-processed ambipolar hosts comprising polymer−polymer or small-molecule-polymer blends, the current polymers may be advantageous in that phase separation between hole-transport and electron-transport components is not possible; although phase separation of the phosphor is still potentially an issue, this should be addressable by copolymerization of phosphor-functionalized monomers, such as those reported in ref 65 with host monomers such as **8**. Moreover, improvements might be anticipated after optimization of layer thicknesses and perhaps variation of the other organic materials. In particular, depending on the location of the recombination zone within the emissive layer, triplet energy transfer to poly-TPD-F (the triplet energy of which is presumably close to the 2.3 eV reported for 4,4′-bis(phenyl-*m*-tolylamino)biphenyl, TPD[52]) could have an adverse effect on the device performance, while if the polymers are to be used as hosts for blue-green phosphors such as FIrpic then BCP ($E_T = 2.5$ eV[52]) may also have to be replaced by a higher-triplet-energy species to effectively confine triplet excitons to the emissive layer.

■ CONCLUSIONS

Polymethacrylates, polystyrenes, and polynorbornenes have been prepared with three different phenylene-linked carbazole-oxadiazole side chains; the polymers exhibit high decomposition temperatures and moderate to high glass-transition temperatures that depend on the identity of both the backbone and the side chain. Spectroscopic and electrochemical data for model small compounds suggest that these polymers should be suitable for use as hosts for green and, at least in some cases, blue-green phosphors. Preliminary unoptimized OLEDs in which these materials are used as hosts for the green phosphor Ir(ppy)$_3$ exhibit external quantum efficiencies of about 10%, suggesting that the use of polymers with pendant ambipolar side chains may be a promising approach to solution-processed phosphorescent OLEDs.

■ ASSOCIATED CONTENT

Ⓢ **Supporting Information.** Figures showing TGA, DSC, phosphorescence, and electrochemical data. This material is available free of charge via the Internet at http://pubs.acs.org.

AUTHOR INFORMATION

Corresponding Author

*E-mail: seth.marder@chemistry.gatech.edu.

ACKNOWLEDGMENT

Support from Solvay SA and from the Science and Technology Center Program of the National Science Foundation (DMR-0120967) is gratefully acknowledged. We are grateful to Jean-Pierre Catinat and Véronique Mathieu for measuring the adiabatic triplet energy of **15**.

REFERENCES

(1) Lamansky, S.; Djurovich, P.; Murphy, D.; Abdel-Razzaq, F.; Lee, H.-E.; Adachi, C.; Burrows, P. E.; Forrest, S. R.; Thompson, M. E. *J. Am. Chem. Soc.* **2001**, *123*, 4304.

(2) Chen, F. C.; Yang, Y.; Thompson, M. E.; Kido, J. *Appl. Phys. Lett.* **2002**, *80*, 2308.

(3) Rudmann, H.; Shimada, S.; Rubner, M. F. *J. Am. Chem. Soc.* **2002**, *124*, 4918.

(4) Gong, X.; Ostrowski, J. C.; Bazan, G. C.; Moses, D.; Heeger, A. J. *Appl. Phys. Lett.* **2002**, *81*, 3711.

(5) Holder, R.; Langeveld, B. M. W.; Schubert, U. S. *Adv. Mater.* **2005**, *17*, 1109.

(6) Chou, P.-T.; Chi, Y. *Chem.—Eur. J.* **2007**, *13*, 380.

(7) So, F.; Krummacher, B.; Mathai, M. K.; Poplavskyy, D.; Choulis, S. A.; Choong, V.-E. *J. Appl. Phys.* **2007**, *102*, 091101.

(8) Kappaun, S.; Slugovc, C.; List, E. J. W. *Int. J. Mol. Sci.* **2008**, *9*, 1527.

(9) Chou, H. H.; Cheng, C. H. *Adv. Mater.* **2010**, *22*, 2468.

(10) Mi, B.-X.; Gao, Z.-Q.; Liao, Z.-J.; Huang, W.; Chen, C. H. *Sci. China, Ser. B: Chem.* **2010**, *53*, 1679.

(11) Xiao, L.; Chen, Z.; Qu, B.; Luo, J.; Kong, S.; Gong, Q.; Kido, J. *Adv. Mater.* **2011**, *23*, 926.

(12) Sasabe, H.; Kido, J. *Chem. Mater.* **2011**, *23*, 621.

(13) Baldo, M. A.; O'Brien, D. F.; You, Y.; Shoustikov, A.; Sibley, S.; Thompson, M. E.; Forrest, S. R. *Nature* **1998**, *395*, 151.

(14) Baldo, M. A.; Adachi, C.; Forrest, S. R. *Phys. Rev. B* **2000**, *62*, 10967.

(15) Burn, P. L.; Lo, S.-C.; Samuel, I. D. W. *Adv. Mater.* **2007**, *19*, 1675.

(16) Giebink, N. C.; Forrest, S. R. *Phys. Rev. B* **2008**, *77*, 235215.

(17) Kim, S. H.; Jang, J.; Yook, K. S.; Lee, J. Y. *Appl. Phys. Lett.* **2008**, *92*, 023513.

(18) Adachi, C.; Kwong, R.; Forrest, S. *Org. Electron.* **2001**, *2*, 37.

(19) Lamansky, S.; Djurovich, P.; Abdel-Razzaq, F.; Garon, S.; Murphy, D.; Thompson, M. E. *J. Appl. Phys.* **2002**, *92*, 1570.

(20) Gong, X.; Ostrowski, J. C.; Moses, D.; Bazan, G. C.; Heeger, A. J. *Adv. Funct. Mater.* **2003**, *13*, 439.

(21) Yang, X. H.; Neher, D. *Appl. Phys. Lett.* **2004**, *84*, 2476.

(22) Yang, X. H.; Jaiser, F.; Klinger, S.; Neher, D. *Appl. Phys. Lett.* **2006**, *88*, 021107.

(23) However, in some cases, given appropriate excited-state lifetimes, reasonably efficient guest-based emission can still be obtained when the guest triplet is slightly higher in energy than that of the host. Adachi, C.; Kwong, R. C.; Djurovich, P. I.; Adamovich, V.; Baldo, M. A.; Thompson, M. E.; Forrest, S. *Appl. Phys. Lett.* **2001**, *79*, 2082.

(24) Yang, X. H.; Müller, D. C.; Neher, D.; Meerholz, K. *Adv. Mater.* **2006**, *18*, 948.

(25) Zhang, K.; Chen, Z.; Yang, C.; Zhang, X.; Tao, Y.; Duan, L.; Chen, L.; Zhu, L.; Qin, J.; Cao, Y. *J. Mater. Chem.* **2007**, *17*, 3451.

(26) Kim, S.-J.; Zhang, Y.; Zuniga, C.; Barlow, S.; Marder, S. R.; Kippelen, B. *Org. Electron.* **2011**, *12*, 492.

(27) Deng, L.; Furuta, P. T.; Garon, S.; Li, J.; Kavulak, D.; Thompson, M. E.; Fréchet, J. M. J. *Chem. Mater.* **2006**, *18*, 386.

(28) Zhang, K.; Tao, Y.; Yang, C.; You, H.; Zou, Y.; Qin, J.; Ma, D. *Chem. Mater.* **2008**, *20*, 7324.

(29) Brunner, K.; van Dijken, A.; Börner, H.; Bastiaansen, J. J. A. M.; Kiggen, N. M. M.; Langeveld, B. M. W. *J. Am. Chem. Soc.* **2004**, *126*, 6035.

(30) Guan, M.; Chen, Z. Q.; Bian, Z. Q.; Liu, Z. W.; Gong, Z. L.; Baik, W.; Lee, H. J.; Huang, C. H. *Org. Electron.* **2006**, *7*, 330.

(31) Leung, M.-k.; Yang, C.-C.; Lee, J.-H.; Tsai, H.-H.; Lin, C.-F.; Huang, C.-Y.; Su, Y. O.; Chiu, C.-F. *Org. Lett.* **2007**, *9*, 235.

(32) Tao, Y.; Wang, Q.; Yang, C.; Wang, Q.; Zhang, Z.; Zou, T.; Qin, J.; Ma, D. *Angew. Chem., Int. Ed.* **2008**, *47*, 8104.

(33) Tao, Y.; Wang, Q.; Yang, C.; Zhong, C.; Zhang, K.; Qin, J.; Ma, D. *Adv. Funct. Mater.* **2010**, *20*, 304.

(34) Jiang, X.; Register, R. A.; Killeen, K. A.; Thompson, M. E.; Pschenitzka, F.; Sturm, J. C. *Chem. Mater.* **2000**, *12*, 2542.

(35) Guan, M.; Bian, Z. Q.; Zhou, Y. F.; Li, F. Y.; Li, Z. J.; Huang, C. H. *Chem. Commun.* **2003**, *2003*, 2708.

(36) Kamtekar, K. T.; Wang, C.; Bettington, S.; Batsanov, A. S.; Perepichka, I. F.; Bryce, M. R.; Ahn, J. H.; Rabinal, M.; Petty, M. C. *J. Mater. Chem.* **2006**, *16*, 3823.

(37) Ding, S.; Tang, H.; Radosz, M.; Shen, Y. *J. Polym. Sci., Part A: Polym. Chem.* **2004**, *42*, 5794.

(38) Stubbs, L. P.; Weck, M. *Chem.—Eur. J.* **2003**, *9*, 992.

(39) Ebert, G. W.; Juda, W. L.; Kosakowski, R. H.; Ma, B.; Dong, L.; Cummings, K. E.; Phelps, M. V.; Mostafa, A. E.; Luo, J. *J. Org. Chem.* **2005**, *70*, 4314.

(40) Li, F.; Yang, S. I.; Ciringh, Y.; Seth, J.; Martin, C. H.; Singh, D. L.; Kim, D.; Birge, R. R.; Bocian, D. F.; Holten, D.; Lindsey, J. S. *J. Am. Chem. Soc.* **1998**, *120*, 10001.

(41) Hreha, R. D.; Haldi, A.; Domercq, B.; Barlow, S.; Kippelen, B.; Marder, S. R. *Tetrahedron* **2004**, *60*, 7169.

(42) Domercq, B.; Hreha, R. D.; Zhang, Y.-D.; Larribeau, N.; Haddock, J. N.; Schultz, C.; Marder, S. R.; Kippelen, B. *Chem. Mater.* **2003**, *15*, 1491.

(43) Hreha, w. D.; Zhang, Y.-D.; Domercq, B.; Larribeau, N.; Haddock, J. N.; Kippelen, B.; Marder, S. R. *Synthesis* **2002**, 1201.

(44) Frisch, M. J.; Trucks, G. W.; Schlegel, H. B.; Scuseria, G. E.; Robb, M. A.; Cheeseman, J. R.; Montgomery, J. A.; Vreven, T.; Kudin, K. N.; Burant, J. C.; Millam, J. M.; Iyengar, S. S.; Tomasi, J.; Barone, V.; Mennucci, B.; Cossi, M.; Scalmani, G.; Rega, N.; Petersson, G. A.; Nakatsuji, H.; Hada, M.; Ehara, M.; Toyota, K.; Fukuda, R.; Hasegawa, J.; Ishida, M.; Nakajima, T.; Honda, Y.; Kitao, O.; Nakai, H.; Klene, M.; Li, X.; Knox, J. E.; Hratchian, H. P.; Cross, J. B.; Bakken, V.; Adamo, C.; Jaramillo, J.; Gomperts, R.; Stratmann, R. E.; Yazyev, O.; Austin, A. J.; Cammi, R.; Pomelli, C.; Ochterski, J. W.; Ayala, P. Y.; Morokuma, K.; Voth, G. A.; Salvador, P.; Dannenberg, J. J.; Zakrzewski, V. G.; Dapprich, S.; Daniels, A. D.; Strain, M. C.; Farkas, O.; Malick, D. K.; Rabuck, A. D.; Raghavachari, K.; Foresman, J. B.; Ortiz, J. V.; Cui, Q.; Baboul, A. G.; Clifford, S.; Cioslowski, J.; Stefanov, B. B.; Liu, G.; Liashenko, A.; Piskorz, P.; Komaromi, I.; Martin, R. L.; Fox, D. J.; Keith, T.; Al-Laham, M. A.; Peng, C. Y.; Nanayakkara, A.; Challacombe, M.; Gill, P. M. W.; Johnson, B.; Chen, W.; Wong, M. W.; Gonzalez, C.; Pople, J. A. *Gaussian03*, Revision E.01; Gaussian Inc.: Wallingford, CT, 2004.

(45) Gamero, V.; Velasco, D.; Latorre, S.; López-Calahorra, F.; Brillas, E.; Juliá, L. *Tetrahedron Lett.* **2006**, *47*, 2305.

(46) Kawaguchi, K.; Nakano, K.; Nozaki2, K. *J. Org. Chem.* **2007**, *72*, 5119.

(47) Kim, J. H.; Yoon, D. Y.; Kim, J. W.; Kim, J.-J. *Synth. Met.* **2007**, *157*, 743.

(48) The orbitals are similar to those shown for **IV** and **V** in ref 33 although those of **V** show more phenylene and oxadiazole contributions to the HOMO than is seen for **IV** or for **13**−**15**.

(49) Shih, P.-I.; Chiang, C.-L.; Dixit, A. K.; Chen, C.-K.; Yuan, M.-C.; Lee, R.-Y.; Chen, C.-T.; Diau, E. W.-G.; Shu, C.-F. *Org. Lett.* **2006**, *8*, 2799.

(50) Values of ca. 3.0 eV are obtained for the meta-linked carbazole-triazoles **VII** and **IX** (see ref 47).

(51) It is interesting also to compare the values of 2.72 eV for **VI** with the 2.56 eV reported for 4,4′-di(carbazol-9-yl)biphenyl (CBP) (ref 52),

of which it can be considered a derivative. Presumably the oxadiazole substitution of **VI** leads to a significant twist of the biphenyl and results in two essentially decoupled **13**-like chromophores.

(52) Baldo, M. A.; Forrest, S. *Phys. Rev. B* **2000**, *62*, 10958.

(53) Endo, A.; Suzuki, K.; Yoshihara, T.; Tobita, S.; Yahiro, M.; Adachi, C. *Chem. Phys. Lett.* **2008**, *460*, 155.

(54) Adachi, C.; Kwong, R. C.; Djurovich, P. I.; Adamovich, V.; Baldo, M. A.; Thompson, M. E.; Forrest, S. *Appl. Phys. Lett.* **2001**, *79*, 2082.

(55) Holmes, R. J.; Forrest, S. R.; Tung, Y.-J.; Kwong, R. C.; Brown, J. J.; Garon, S.; Thompson, M. E. *Appl. Phys. Lett.* **2003**, *82*, 2422.

(56) Ambrose, J. F.; Nelson, R. F. *J. Electrochem. Soc.* **1968**, *115*, 1159.

(57) Ambrose, J. F.; Carpenter, L. L.; Nelson, R. F. *J. Electrochem. Soc.* **1975**, *122*, 876.

(58) Keszthelyi, C. P.; Tachikawa, H.; Bard, A. J. *J. Am. Chem. Soc.* **1972**, *94*, 1522.

(59) Obtained from the value quoted vs. SCE in ref 58 by using a value of +0.40 V vs. SCE for the $FeCp_2^{+/0}$ couple in MeCN/0.1 M $^{n}Bu_4NPF_6$. Connelly, N. G.; Geiger, W. E. *Chem. Rev.* **1996**, *96*, 877.

(60) Pommerehne, J.; Vestweber, H.; Guss, W.; Mahrt, R. F.; Bässler, H.; Porsch, M.; Daub, J. *Adv. Mater.* **1995**, *7*, 551.

(61) Solid-state and gas-phase IPs often differ by 1 eV or more because of solid-state polarization effects; see, for example, Anderson, J. D.; McDonald, E. M.; Lee, P. A.; Anderson, M. L.; Ritchie, E. L.; Hall, H. K.; Hopkins, T.; Nash, E. A.; Wang, J.; Padias, A.; Thayumanavan, S.; Barlow, S.; Marder, S. R.; Jabbour, G.; Shaheen, S.; Kippelen, B.; Peyghambarian, N.; Wightman, R. M.; Armstrong, N. R. *J. Am. Chem. Soc.* **1998**, *120*, 9646. Similar effects are expected for EAs.

(62) Haldi, A.; Kimyonok, A.; Domercq, B.; Hayden, L. E.; Jones, S. C.; Marder, S. R.; Weck, M.; Kippelen, B. *Adv. Funct. Mater.* **2008**, *18*, 3056.

(63) Zhan, X.; Haldi, A.; Yu, J.; Kondo, T.; Domercq, B.; Cho, J.-Y.; Barlow, S.; Kippelen, B.; Marder, S. R. *Polymer* **2009**, *50*, 397.

(64) In ref 26 we also describe somewhat more efficient devices (EQE up to 13.6%) in which the related more soluble $Ir(pppy)_3$ is used in place of $Ir(ppy)_3$.

(65) Kimyonok, A.; Domercq, B.; Haldi, A.; Cho, J.-Y.; Carlise, J. R.; Wang, X.-Y.; Hayden, L. E.; Jones, S. C.; Barlow, S.; Marder, S. R.; Kippelen, B.; Weck, M. *Chem. Mater.* **2007**, *19*, 5602.